Fire From Volcanic Activity: Quantifying the threat from an understudied hazard

Jia Yong Quah[a], Josh L. Hayes[b,c], Rebecca H. Fitzgerald[c,d], Geoffrey A. Lerner[b,e], Susanna F. Jenkins[a,b], Thomas M. Wilson[d], Finn Scheele[c], Biljana Lukovic[c], Charles Fleischmann[f]

[a]Asian School of the Environment, Nanyang Technological University, Singapore

[b]Earth Observatory of Singapore, Nanyang Technological University, Singapore

[c]GNS Science, Lower Hutt, New Zealand

[d]School of Earth and Environment, University of Canterbury, Christchurch, New Zealand

[e]Instituto de Geofísica, Universidad Nacional Autónoma de Mexico, Mexico City, Mexico

[f]Department of Civil and Natural Resources Engineering, University of Canterbury, Christchurch, New Zealand

Corresponding author: Geoffrey Lerner (glerner@igeofisica.unam.mx)

October 29, 2022

This manuscript is a non-peer reviewed preprint submitted to the International Journal of Disaster Risk Reduction and has not yet been accepted for publication. Subsequent versions of this manuscript may have different content. If accepted, the final version of this manuscript will be available via the 'Peer-reviewed Publication DOI' link on its EarthArXiv web page. Please feel free to contact us with any comments or feedback about our study.

Abstract

Fire from volcanic activity (FFVA) is a highly dangerous and largely understudied hazard arising from volcanic activity. FFVA can be caused by a variety of volcanic hazards and can greatly compound the damage and losses associated with volcanic activity, in addition to creating complications for event response and mitigation. In this study, we develop a FFVA ignition probability model underpinned by a widely applicable fault tree, which identifies the mechanisms that can lead to fire ignition from volcanic activity. By assigning values to each node of the fault tree, our model can be used to consider the relative probabilities associated with different fire ignition mechanisms. We couple this model with a fire spread model to evaluate hazardous areas and associated impacts caused by FFVA. To demonstrate the

applicability of our model, we use an eruption scenario for volcanic ballistic projectiles (VBPs) in the Auckland Volcanic Field (Aotearoa New Zealand). We found that burn zones were highly sensitive to wind conditions and fuel availability. The maximum credible damaging wind permutation for VBP-ignited FFVA in Auckland results in over NZ$3.9 billion damage to buildings and infrastructure, four times greater than if fire spread was not considered. This case study demonstrates the potential for FFVA to compound and greatly increase the impacts caused by other volcanic hazards and we suggest that more study is needed to better understand, evaluate and plan for FFVA.

Keywords: fire, eruption, hazard, fault tree, ballistic, Auckland

1 Introduction

Fires associated with natural hazards, like earthquakes and volcanic eruptions, can cause major impacts to both humans and the built environment. They can expand the area and assets impacted by the initiating hazard through fire spread and/or compound the severity of impacts for already damaged assets (e.g., a lightly damaged house becoming a complete loss due to fire damage) (Scawthorn et al., 2005). Considerable research has been undertaken to understand and model ignition processes, spread, and cascading effects of fire following earthquakes, which has led to improved understanding of vulnerabilities in urban areas, building engineering, and mitigation tactics (e.g., Lee et al., 2008; Zolfaghari et al., 2009; Scawthorn, 2018; Suwondo et al., 2019; Coar et al., 2021). However, little work has focused on the potential for fire from volcanic activity, despite a number of prominent historical examples. For example, pyroclastic density currents (PDCs) in the 1902 eruption of Mt. Pelée ignited ships in the harbour and caused widespread fires that destroyed the entire city of St. Pierre, Martinique (Tanguy, 1994). Additionally, PDCs from the 1997 eruption of Soufrière Hills volcano (Montserrat) and the 2010 eruption of Merapi (Indonesia) caused heavy fire damage to building interiors and entire buildings in several villages (Baxter et al., 2005; Jenkins et al., 2013). During several eruptions, including 1783 Asama (Japan), 1914 Sakurajima (Japan), and 2010 Pacaya (Guatemala), volcanic ballistic projectiles (VBP) pierced building roofs, leading to ignition of buildings and in some cases widespread fire (Blong, 1984; Wardman et al., 2012b). Lava flows from the 2018 Lower East Rift Zone eruption at Kīlauea volcano, Hawai'i caused damage to structures by directly igniting buildings or by fire spread, affecting buildings up to 600 m from the flow margins (Meredith et al., 2022).

While the threat posed by fires during or in the aftermath of volcanic activity has been acknowledged in a small number of works (e.g., Blong, 1984; Jenkins et al., 2014; Wilson et al., 2014), it has rarely been the centre of a study or quantitatively modelled to provide fire-related impact or loss estimates. A small group of studies have explicitly considered damage caused by fire following PDCs. Baxter et al. (2005) studied building damage associated with fires ignited by high-energy dilute PDC deposits during the 1997 eruption of Soufrière Hills volcano, Montserrat, and Jenkins et al. (2013) and Lerner et al. (2022) assessed building damage from fires ignited by embers carried within low-energy dilute PDCs during the 2010 Merapi eruption. Studies of the 2014-15 eruption of Fogo (Cape Verde; Jenkins et al., 2017) and 2018 eruption of Kīlauea (Hawaii; Meredith et al., 2022) eruptions have also considered fires resulting from lava flows in their post-eruption impact assessments. Only one known study (unpublished) has aimed to model the potential fire hazard from volcanic eruptions (with a focus on tephra fall, PDCs, and volcanic earthquakes) by assessing probabilities of fire ignition, spread, and human survival following a hypothetical eruption of Vesuvius, Italy (Jenkins et al., 2009).

Fire from volcanic activity (FFVA) differs from the more extensively studied fire following earthquakes (FFE) in a number of critical ways. While ignitions (combustion and the presence of a flame) of FFE are typically indirect (e.g., electrical short circuits, gas pipe ruptures) (Scawthorn, 1986), volcanic hazards such as tephra fall, PDC, lava flows, and VBP can start fires through a variety of both direct (contact or proximity with high-temperature hazards) and indirect (related to physical properties of the volcanic material or hazard other than temperature, e.g., abrasive properties, mechanical impact) ignitions (Tables 1 and 2). Further, volcanic eruptions can sometimes be forecast with sufficient time for mitigation activities to be undertaken to reduce fire risk. For example, removal of flammable materials can be undertaken before an eruption commences or before inundation by hazardous volcanic phenomena, such as lava flows (Jenkins et al., 2017; Meredith et al., 2022). Other mitigation actions include boarding up windows prior to PDC invasion (Baxter et al., 2005) and using corrugated steel to reduce the risk of hot ballistics smashing windows and landing inside buildings, with the aim of reducing the potential for building contents (e.g., carpets and furniture) to ignite (Williams and Moore, 1983).

Fire spread from FFVA, however, is also subject to many of the same conditions as fire spread following other disasters. Environmental factors such as high winds, availability of fuel (human-made or vegetation), and prolonged dry conditions can increase the likelihood of fire ignition and spread (Lee et al., 2008). Damage and disruption to critical infrastructure during disasters can hinder fire suppression efforts, which can increase the destructiveness of subsequent fires (Gernay and Khorasani, 2019). Such disruption can occur during volcanic eruptions through disturbance of road networks from burial by flows, reduced traction/visibility from tephra fall, cracks from ground deformation, and/or building or infrastructure damage blocking the road, limiting access for emergency responders to fire sites (Blake et al., 2017), whilst electricity and water supply disruption can limit capacity of emergency responders to fight the fire (Stewart et al., 2006; Wardman et al., 2012a; Wilson et al., 2012; Wilson et al., 2014, 2017). Thus, a better understanding of the potential for FFVA is an important consideration for emergency management and disaster planning. However, no study has taken a whole assessment approach from probability of ignition through to fire and fire spread and the potential losses that may occur.

Table 1: Observed ignition of FFVA damage to the built environment

Volcanic hazard	Temperature (upper range) (°C)	Mechanism	Examples
Volcanic ballistic projectiles (VBP)	Starting temperature up to 1050 ℃. Solidified fragments up to 600-800 ℃. (Blong, 1984; Alvarado et al., 2006; Vanderkluysen et al., 2012)	• Direct building ignition from high temperatures (Blong, 1984) • Perforation and ignition of building contents (Wardman et al., 2012b)	• 1783 Asama, Japan (Blong, 1984) • 1914 Sakurajima, Japan (Blong, 1984) • 2007 Stromboli (Pistolesi et al., 2011) • 2010 Pacaya, Guatemala (Wardman et al., 2012b)
Pyroclastic density currents (PDC)	Commonly 200-600 ℃, up to 1100 ℃ (Brown and Andrews, 2015)	• Direct ignition of buildings due to high temperature of PDC and associated deposits (Baxter et al., 2005; Zuccaro et al., 2015; Turchi et al., 2020) • Dynamic pressure from PDC and entrained projectiles breaching the building. Building content ignited directly by hot deposits. • Breaching of a building not always necessary for high temperatures inside the building. In a surge, hot ash or embers have been reported to seep through small gaps, burning victims (Baxter, 1990) and igniting building contents (Jenkins et al., 2013). • High temperatures from PDCs can ignite fuel tanks, which can explode leading to more widespread fires (Jenkins et al., 2016)	• 1902 Mt. Pelée, Martinique (Lacroix, 1904; Hovey, 1904) • 1991 Unzen, Japan (Nakada et al., 1999) • 1997 Soufrière Hills, Montserrat (Baxter et al., 2005) • 2010 Merapi, Indonesia (Jenkins et al., 2013) • 2018 Fuego, Guatemala (Lerner et al., 2022)
Lava flows	700-1200 ℃ (Kilburn, 2015)	• Direct ignition of buildings and fuel tanks by radiation or conduction (Blong, 1984; Ainsworth and Boone Kauffman, 2009; Harris, 2015; Jenkins et al., 2017; Meredith et al. 2022)	• 1973 Heimaey, Iceland (Williams and Moore, 1983) • 2005 Sierra Negra, Galápagos, Ecuador (Geist et al., 2008) • 2014-2015 Fogo, Cabo Verde (Jenkins et al., 2017) • 2018 Kīlauea, Hawaii, USA (Meredith et al., 2022)

Table 2: Credible theoretical causes of ignition of FFVA in the built environment. Ignition of vegetation or other flammable material (e.g., animal feed, firewood, outdoor furniture) close to buildings can result in ignition of a building through fire spread or radiant heat.

Volcanic hazard	Mechanism
Tephra fall	• Block filters and fans of appliances/electrical equipment, resulting in overheating (Wilson et al., 2014) • Dusting of magnetic, conductive, abrasive tephra on electronic components (especially if the tephra is moist i.e., low resistivity or/and accompanied by acidic aerosols), resulting in failure of the equipment or malfunction, insulator flashover for electrical supply networks (e.g., Gordon et al., 2005, Wilson and Cole, 2007, Wardman et al., 2012b, Wilson et al., 2014). Discharges during the flashover process can reach temperatures of >3000 °C, significantly higher than the ignition temperature of timber (500 °C) (Genareau et al., 2015). • Abrasion of electrical wirings resulting in short circuit
Volcanic ballistic projectiles (VBP)	• Breaking of power lines/electrical equipment resulting in malfunction
Pyroclastic density currents (PDC)	• Ignition as PDC breaches the building and results in electrical equipment abrasion and/or malfunction (similar to tephra fall) (Wilson et al., 2014)
Lava flows	• Mechanical damage to buildings and assets (e.g., electrical equipment) resulting in malfunction • Rupture of gas lines
Ground deformation	• Rupture of gas lines resulting in leaked fuel • Damage of underground electrical cables leading to short circuits
Volcanic earthquakes	• Ground shaking causing breakage or overturning of building contents that may explode or create short circuits or arcing, • Abrasion or other damage to electrical wiring from excessive structural deflections • Rupture of gas piping (Scawthorn, 1986) • Less typical but observed modes of ignitions are heating due to friction or sparking due to the pounding of structures (Scawthorn, 1986).
Volcanogenic lightning	• Direct ignition from lightning strike (Temperatures up to 29,727 ℃; Genareau et al., 2017)

In this study, we develop a framework for assessing FFVA hazard using a fault tree, which identifies branches of potential contributing factors that can lead to a "fault", in this case fire ignition. This fault tree accounts for ignition due to most types of volcanic hazards and can be adapted into an ignition model for FFVA resulting from specific hazards and paired with a fire spread model to serve as a framework for evaluating potential FFVA damage. We use our framework to assess the potential for FFVA damage resulting from VBP during an Auckland Volcanic Field (AVF) eruption scenario. We then use this case study to identify potential factors and issues associated with FFVA broadly and in the AVF.

2 FFVA Framework

In this study we developed a generalized framework for analysing FFVA that can be tailored to suit various eruption scenarios, assets, and volcanic hazards. The framework begins with a fault tree to characterize the interactions of the potential ignition sources from any of the major volcanic hazards with components of the asset being considered (e.g., a building), based on mechanisms of fire ignition observed in past events (Table 1) and our knowledge of hazard-component interaction (Table 2). The second part of the framework involves creating an ignition model by adapting the fault tree for the volcanic hazard and particular asset being considered and using available data and expert judgement to quantify ignition probabilities. We then combine our ignition model with a fire spread model (Cousins et al., 2002), which can then be adapted to account for the hazard, environmental conditions, such as wind direction and speed, and characteristics of the built environment under consideration, such as building density and typology.

In the below sections, we discuss how each of these conceptual elements can be captured within a risk assessment framework that combines hazard, exposure, and vulnerability information (e.g., Simpson et al. 2014). First, we present an overview of our generalized FFVA ignition fault tree, which is applicable for multiple different volcanic hazards. Following this, we show how the generalized fault tree can be adapted to create an ignition model for volcanic ballistic projectiles. We then describe the fire spread model that supports our framework.

2.1 FFVA ignition fault tree

We developed a fault tree that evaluates the conditions that could lead to FFVA of a single-storey residential house. We chose a single-storey residential house to avoid the design- and system-specific characteristics of industrial, commercial or high-rise buildings or infrastructure that would affect ignition, although we recognize that these are important areas for future research. A fault tree is a logic-based graph representing combinations of failure or malfunction events in a complex system and the consequences of these failures for the functionality of the system as a whole (Youance et al., 2012). The fault tree lays out the relationship among events, making it possible to simplify and identify failure scenarios in order to better understand the relationship between volcanic activity and FFVA. Fault trees can be qualitative or quantitative (Paté-Cornell, 1984) and have been widely used to evaluate FFE (e.g., Williamson and Groner, 2000; Zolfaghari et al., 2009; Youance et al., 2012; Yildiz and Karaman, 2013; Ju, 2016). Our FFVA ignition fault tree was informed by existing fault trees for FFE, by identifying fire ignition sources that are common to both earthquakes and volcanic eruptions (informed by Tables 1 and 2).

In our fault tree (Figure 1), we lay out the interactions we identified between different hazards and house components. We split a house into component parts to evaluate how different interactions between hazards and each component part can lead to ignition and fire spread. The fault tree is based upon three fundamental requirements for a fire: fuel (house or objects in/near the house), a source for ignition (ranging from direct ignition by the hazard to indirect ignition through equipment malfunction), and heat transfer from the ignition to the fuel. From the fault tree, it is possible to focus on the pathways of a particular hazard to potential impacts. The junctions of the tree are separated by either an 'AND' gate or an 'OR' gate, which defines the conditions for the outcome above the gate. For the fault event above an 'OR' gate to happen, *any* of the base events passing through the gate must be true. For the fault event above an 'AND' gate to happen, *all* the base events passing through the gate must be true. For example, in our fault tree (Figure 1), the "Roof on Fire" fault event is true if an ignition source is present 'AND' there is sufficient heat transfer 'AND' there is sufficient availability of fuel. By contrast, the "Residential House on Fire" fault event is true if the roof 'OR' the walls 'OR' the building contents 'OR' the front porch is on fire.

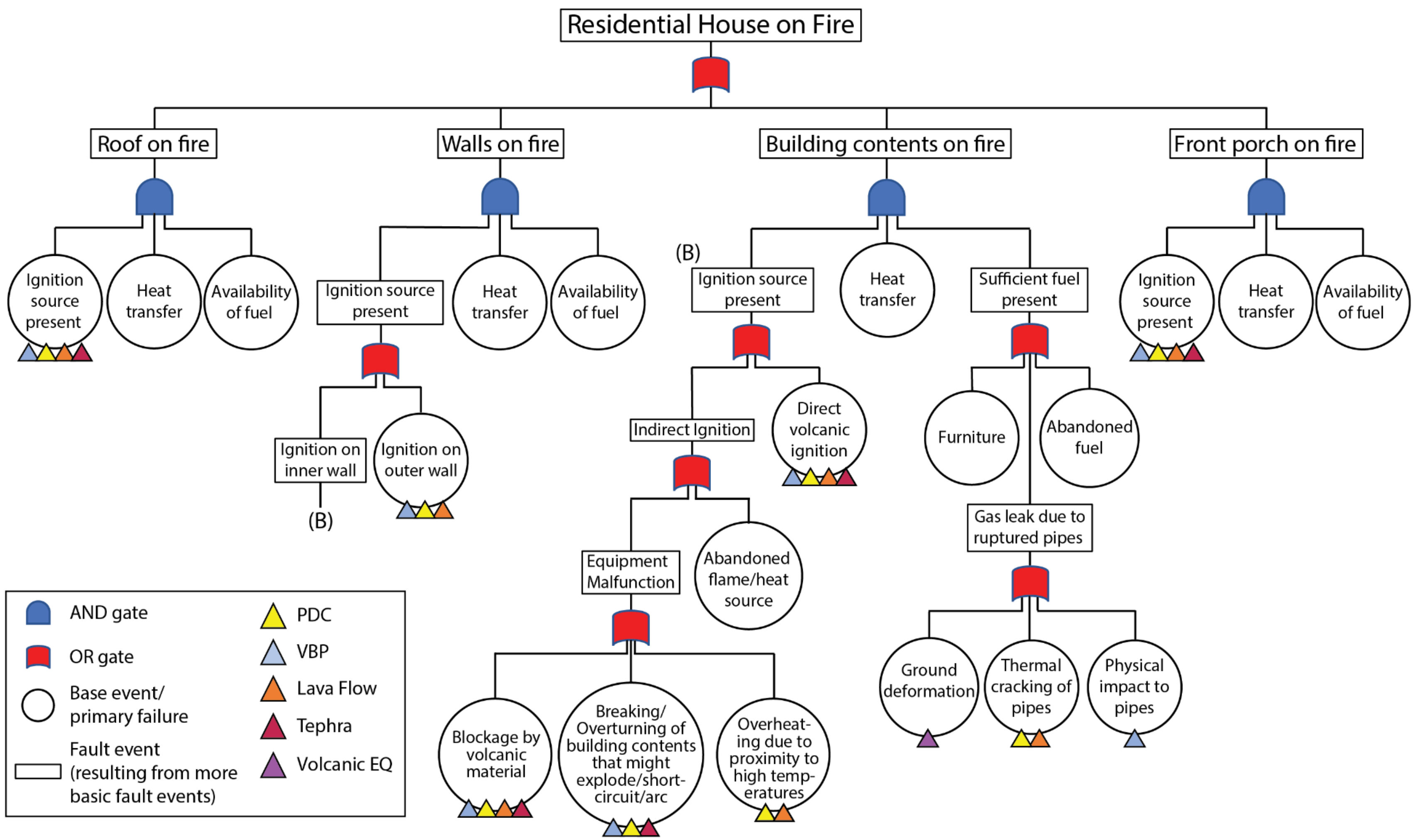

Figure 1. *Fault tree representing how interaction between different volcanic hazards and the different components of a typical single-storey residential home can lead to ignition. The "Ignition on inner wall" fault path ending in (B) continues with an identical path to the "Ignition source present" fault event labelled (B).*

The FFVA fault tree (Figure 1) provides a visual representation of how different ignitions or system failures can either directly lead to a residential house catching fire or interact with each other to have the same outcome. The 'AND' gate that leads to each individual part of the house being on fire demonstrates that for this to take place, all three inputs must be present. It also provides a framework for calculating the probabilities of each path, allowing the user to identify vulnerabilities where mitigation actions would most effectively limit the probability of ignition. The tree can be modified and potentially expanded to consider other assets, such as multi-storey apartment blocks, critical infrastructure or industrial assets, and can conversely be adapted to focus on one particular scenario and hazard.

2.2 Ignition model

To allow application of the fault tree to a given FFVA scenario, the generalized fault tree can be simplified and adapted to suit the relevant volcanic hazard. This adapted fault tree is used to define an ignition model for the hazard. Here, we demonstrate the use of the fault tree to evaluate VBP hazard (Figure 2). VBP are an ideal hazard for demonstrating fault tree adaptation since their mechanisms for igniting fires are typically direct physical processes that can be clearly quantified into a series of probabilistic equations. In what follows, we present our adapted VBP FFVA fault tree and describe the equations used to create our ignition model.

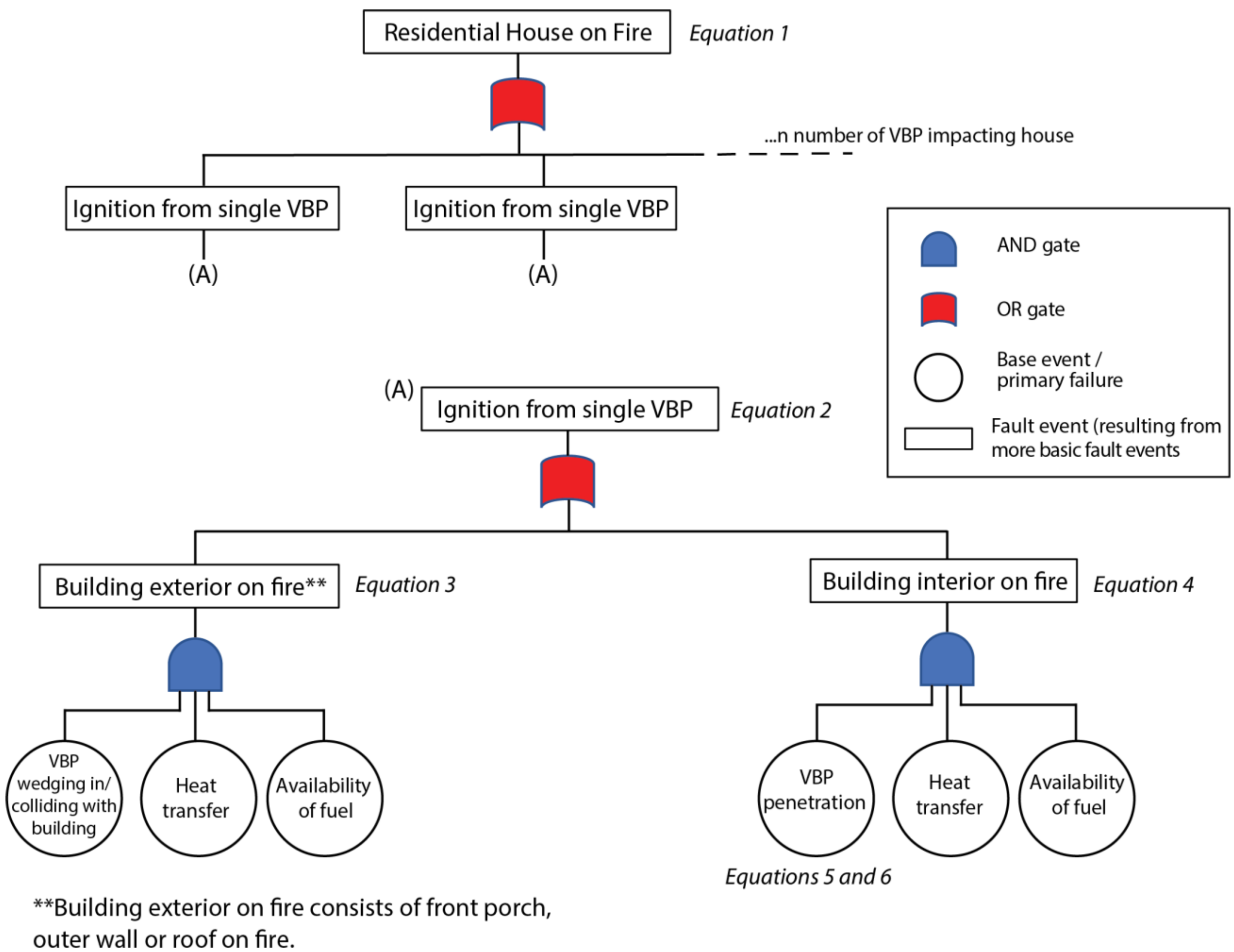

Figure 2. *Simplified fault tree for ignition due to VBP. The probability of a single-storey residential house igniting (the top event) is the sum of probabilities of ignition of all the VBP that land on the building footprint.*

Buildings can be affected by multiple VBPs, so the probability of ignition for a single building (the top level of the fault tree) is equal to the cumulative probability of ignition of all VBPs impacting the building:

$P(i_h) = \sum_{k=0}^{n} P(i_{VBP})$ (Equation 1)

Where: $P(i_h)$ is the probability of the considered house igniting, and $P(i_{VBP})$ is the probability of any given VBP hitting the house and causing ignition. In the model, the buildings are broken into two components, exterior (e.g., front porch, outer wall, roof) and interior (e.g., inner walls, furniture, other contents) to assess the probability of ignition. Whether the interior or exterior of a building is the site of ignition depends on the probability of the ballistic perforating through the roof or walls of a building. The individual probability of ignition from each VBP is determined from summing the probabilities of the two building components being on fire:

$P(i_{VBP}) = P\left(i_{VBP_{exterior}}\right) + (i_{VBP_{interior}})$ (Equation 2)

Where: $P(i_{VBP_{exterior}})$ is the probability of the VBP igniting the exterior of the building, and $P(i_{VBP_{interior}})$ is the probability of the ballistic igniting the interior of the building. The building exterior is subject to ignition from VBPs which fail to perforate the roof and/or walls, while the building interior is subject to ignition from VBPs that do perforate the roof and/or wall. Whether any given ballistic ignites the interior or exterior of a given building is dependent upon the probability of the VBP perforating the building exterior, deposition temperature of the VBP, and the availability of a fuel source (Equations 3 and 4).

$P\left(i_{VBP_{exterior}}\right) = [1 - P(p_{VBP})] \times P(ht_{VBP}) \times P(af)$ (Equation 3)

$P\left(i_{VBP_{interior}}\right) = P(p_{VBP}) \times P(ht_{VBP}) \times P(af)$ (Equation 4)

Where: $P(p_{VBP})$ is the probability that any given VBP will perforate a building, $P(ht_{VBP})$ is the probability of heat transfer sufficient to cause ignition, and $P(af)$ is the probability of available fuel.

Whether the VBP perforates the building (i.e., roof or walls) depends on landing location, kinetic energy of the VBP, and type of building material being impacted. The landing location and kinetic energy can be obtained from VBP hazard models such as Ballista (Tsunematsu et al., 2016) and Eject! (Mastin, 2001). The types of building materials can be obtained from building typology databases. Then, using VBP vulnerability models that relate hazard intensity to damage severity (e.g., Williams et al. 2017), it is possible to calculate the probability of any given VBP perforating the building material it lands on.

$P(ht_{VBP})$ refers to the probability that there is sufficient heat transfer from the ignition source to ignite the fuel. Therefore, it is necessary to consider the modes of heat transfer and factors that may influence heat transfer such as maximum temperature of VBP, cooling rate, contact area, and duration of contact. For ignition from VBPs, the likely modes of heat transfer are predominantly conduction and, to a lesser extent, radiation. Such probabilities can be obtained by constructing temperature-ignition curves.

$P(af)$ is the probability that fuel is available and accounts for building materials having different susceptibilities for ignition. For example, due to the material composition, timber-framed buildings are assigned a higher probability of available fuel than a reinforced concrete building (assuming all other elements such as building contents are equal) as timber is more susceptible to ignition than reinforced concrete, which is typically considered non-combustible (Scheele et al., 2019).

To operationalise the fault tree within our model, for each ignition probability, we considered the path to be positive if a randomly and uniformly sampled number between 0 and 1 was equal to or lower than the calculated ignition probability.

2.3 Fire spread model

Once the probability of ignition from a chosen hazard has been defined, the next step is to determine to what extent that fire would spread from the points of ignition. Fire spread models attempt to reproduce fire behaviour, such as direction and speed of spread and total burn zone (the area affected by fire). Fire spread models used in FFE are typically GIS-based simulations using physics-based equations to estimate the burn area (Scheele and Horspool, 2018). Models typically consider characteristics of the built environment, ignition locations, and wind conditions but not topography or vegetation.

We are not aware of any fire spread model developed specifically for volcanic eruption-induced fire spread. However, given that most volcanic hazards have the potential to spread in multiple directions in variable quantities (e.g., multiple PDC pulses on different volcano flanks, variable number of ballistics, lava flows impacting buildings in varying locations) and impact potentially combustible objects, fire spread models will need to be able to account for multiple ignition sites from which the fire could spread. One such model was produced by Cousins et al. (2002). The model uses the maximum distance a fire can spread from one building to another under prevailing wind speed and direction (known as the critical separation distance: CSD) to model fire spread (Cousins et al., 2002; Scheele et al., 2019, Cicione et al., 2021; Wang et al., 2021). CSD is directly proportional to wind speed (Table 3) and is represented in the model as a buffer which is created around an ignited building and extended in the direction of the wind until the CSD is reached. In the model, fire is considered to spread to all combustible buildings (i.e., made from material that is defined as combustible in the model) within the CSD buffer of any building that is already on fire. Fire repeatedly spreads to all buildings within the CSD buffer of each ignited building until no new buildings are within the buffer, at which point fire spread is stopped. The fire spread model is further described in the schematic in Figure 3. Once the ignition points are determined using the results of the ignition model, the fire spread model is run multiple times for each permutation of likely wind speed and direction in order to capture relevant permutations.

Table 3: Relationship between wind speed and critical separation distance (after Scheele et al., 2019)

Wind speed (km/h)	Critical Separation Distance (m)
0 – 4.9	12
5 – 9.9	13
10 – 14.9	13
15 – 19.9	14
20 – 24.9	16
25 – 29.9	18
30 – 34.9	23
35 – 39.9	28
40 – 44.9	33
45 – 49.9	42
50 +	45

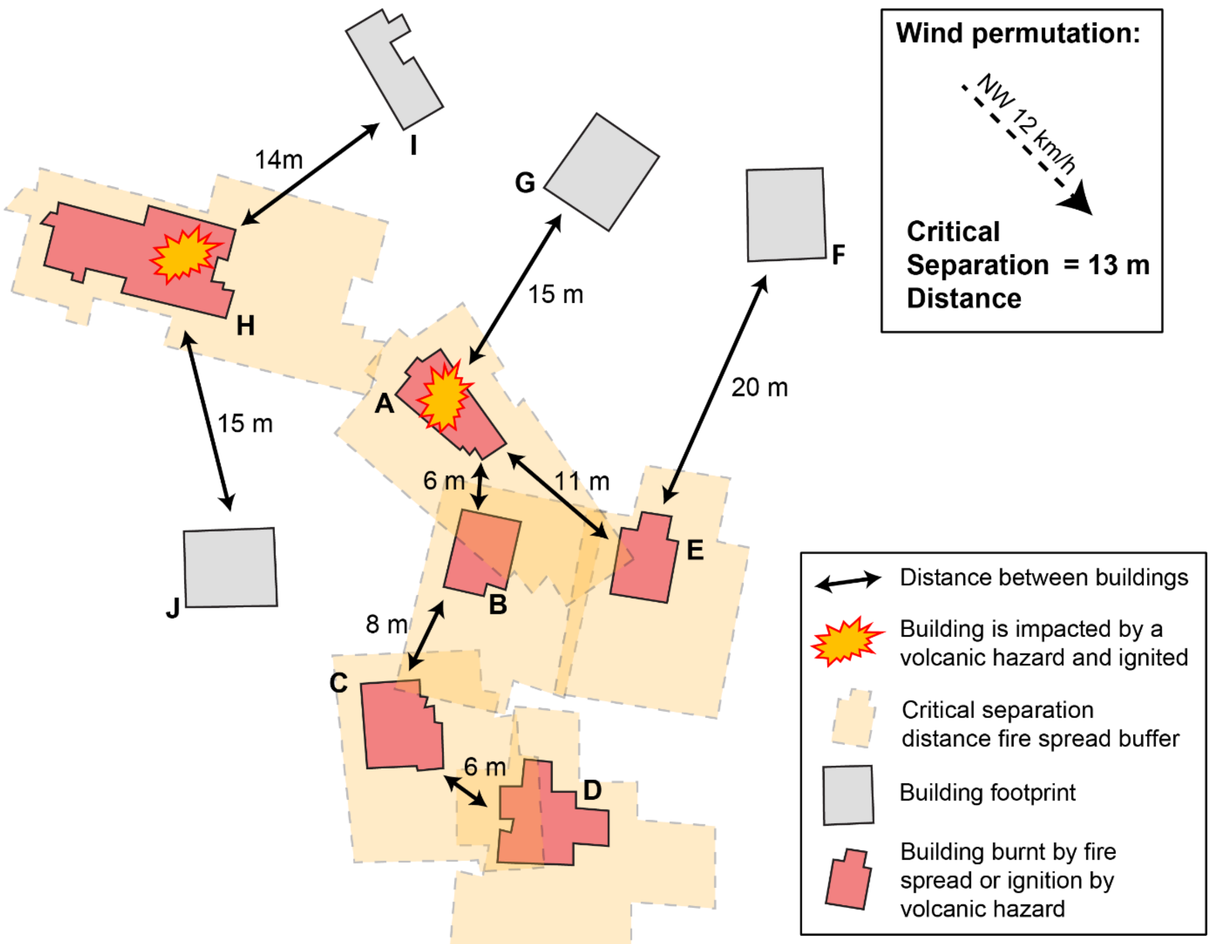

Figure 3. *Schematic cartoon of a fire spread model applied to a volcanic eruption using an example permutation with a critical separation distance (CSD) of 13 m. In this example, buildings A and H are ignited as a result of contact with a volcanic hazard. Fire spreads from building A to B and E due to the overlap of the building A CSD buffer with the boundaries of buildings B and E. Fire continues to spread from B to C to D due to the buffer-building overlap, however fire cannot spread from E to F, A to G, or H to I and J, due to distances between buildings that result in no overlap between the unburnt buildings and the CSD buffer.*

3 Application of modelling framework to Auckland, Aotearoa New Zealand

Having developed a method and framework for evaluating FFVA, we then applied the model to a case study to demonstrate how the generalized fault tree can be adapted to address FFVA hazard in specific wind permutations. We chose to apply our framework to a potential eruption in Auckland, Aotearoa New Zealand (hereafter ANZ), focusing on the VBP hazard. To do so, we used the adapted VBP fault tree described in Section 2.2 and derived probabilities for ignition due to VBP impact that were specific to residential building stock in Auckland. This was coupled with a fire spread model to evaluate potential damage due to FFVA resulting from VBP impact in Auckland. To capture the full potential for FFVA in Auckland, we would need to expand to consider all potential hazards, eruption locations, and scenarios, but for this illustrative application we confine our study to just one hazard scenario, although we do consider FFVA as a function of the potential range of wind conditions.

3.1 Auckland Volcanic Field and scenarios

Auckland is the most populous city in ANZ with over 1.7 million people. It is also an economic centre, responsible for over a third of the nation's Gross Domestic Product (Stats NZ, 2020, 2021). The majority of the city is built on top of the AVF, a monogenetic volcanic field that has been active since 190 ka BP, with the most recent activity taking place ~550 BP (Needham et al., 2011; Leonard et al., 2017; Hopkins et al., 2021). The field covers an area of 360 km^2 and has produced at least 53 separate vents over the course of its eruptive history, representing explosive (magmatic and phreatomagmatic) and effusive eruption styles (Hopkins et al., 2021). New activity is expected in the future, likely to take place from a new vent either on land or in the underwater areas that lie within the field (Runge et al. 2015; Hopkins et al. 2021). No spatiotemporal pattern has been detected among the 53 prior eruptive centres, rendering the location of a future eruption uncertain (Bebbington and Cronin, 2011; Hopkins et al. 2021). Due to the high exposure to volcanic hazards, it is anticipated that impacts from eruptions in the AVF could be severe and may cost billions of dollars in direct (e.g., building damage) and indirect (clean-up and business interruption) losses (Magill et al., 2006; Deligne et al. 2017b; Hayes et al., 2017; McDonald et al. 2017). Thus, a key question is whether any potential fire during or following a potential future AVF eruption could have a tangible influence on potential impact area, losses, and emergency management strategies.

To prepare for future eruptions, the Determining Volcanic Risk in Auckland program (DEVORA) developed eight eruption scenarios that represent a range of possible vent locations, eruption styles, durations, and hazards (Hayes et al., 2020). These scenarios can be used to evaluate the impacts of different hazards in the case of eruption, with Ang et al. (2020) providing their relative probability of occurrence across the AVF. In this study, we use one of these scenarios at one location (DEVORA Scenario D - Mt. Eden suburb) to investigate whether FFVA has the potential to be a considerable threat requiring consideration in Auckland. The scenario involves 320 days of activity, with fire fountaining from 3 vents along a fissure for 7 days, followed by Strombolian eruptions for the next 73 days, and culminating in 240 days of lava effusion (Hayes et al. 2018). The scenario is ideal as a case study for three main reasons: i) it is a land-based, magmatic eruption (i.e., relatively hot eruptive products near buildings); ii) VBP are produced providing possible ignition sources for fires; and iii) it occurs in a primarily residential area, which increases the uniformity of the building types involved, and reduces model complexity for our exploratory analysis.

3.2 Input datasets and modelling procedure

The VBP scenario was modelled using the ballistic trajectory model Ballista (Tsunematsu et al., 2016) to obtain the surficial distribution and mass, diameter, velocity, horizontal distance travelled and impact angle of VBP for Scenario D. The specific modelling parameters used to model the landing and impact energies can be found in Hayes et al. (2018). The eruption scenario is characterised as a long-lasting magmatic eruption. In this study, we used Day 8 to 21 of the scenario, in which Strombolian eruptions occur. In order to focus on FFVA related specifically to VBP, potential impacts to buildings during days 1-7 of the scenario (Hawaiian eruptions) were ignored. VBP landing locations were kept constant across all our FFVA simulations.

VBP temperature is an important variable for ignition models as it defines the probability of sufficient heat transfer and ignition of a building element. What is important is the temperature upon landing on a building element. As ballistics are ejected, they will cool typically at some rate from an initial temperature when travelling through the air (Thomas and Sparks, 1992). Here we calculated VBP cooling rates based on the physico-mathematical model of Capaccioni and Cuccoli (2005) due to complementary clast sizes and travel durations between their model and DEVORA Scenario D.

The RiskScape comprehensive point-based building inventory database was used to determine the location, types, and replacement costs of buildings in Auckland (RiskScape building database 1.0, Sourced from GNS Science with permission; accessed 2 Nov 2020). RiskScape is a risk modelling tool widely used in ANZ (Deligne et al., 2017b; Crawford et al., 2018; Paulik et al., 2022). We then joined the point data with Land Information New Zealand (LINZ) building footprints obtained from aerial imagery (sourced from the LINZ Data Service and licensed for reuse under CC BY 4.0; accessed 18 Nov 2020) to give geolocated building information. Building data from RiskScape were manually cleaned using property boundary data (LINZ, 2014; accessed 19 Nov 2020) to correct outdated building location information, correct misplaced building points, and otherwise ensure that the GIS base for the model was up to date.

All inputs were incorporated first into the ignition model, then with the ignition probability data into the fire spread model, which was run 50 times for each permutation of wind speed (km/hr) and direction (Figure 4). We used 10-minute averaged hourly wind data recorded from 1993 to 2002 at Auckland Airport (National Institute of Water and Atmospheric Research (NIWA) CliFlo database, https://cliflo.niwa.co.nz/; accessed 2 Nov 2020), with wind directions then binned into one of eight directions: N, E, S, W represent winds +/- 25° from each compass bearing while NE, SE, SW, NW represent winds +/- 20° (Figure 5). Wind speeds were reflected in the CSD used to model fire spread (10 CSD values, Table 3 and Figure 5), to give a total of 80 unique wind speed and direction permutations. Thus, we ran a total of 4,000 model simulations. In the below subsections, and summarised in Figure 4, we detail our approach for estimating each of the case study model parameters used in the fire ignition and spread models.

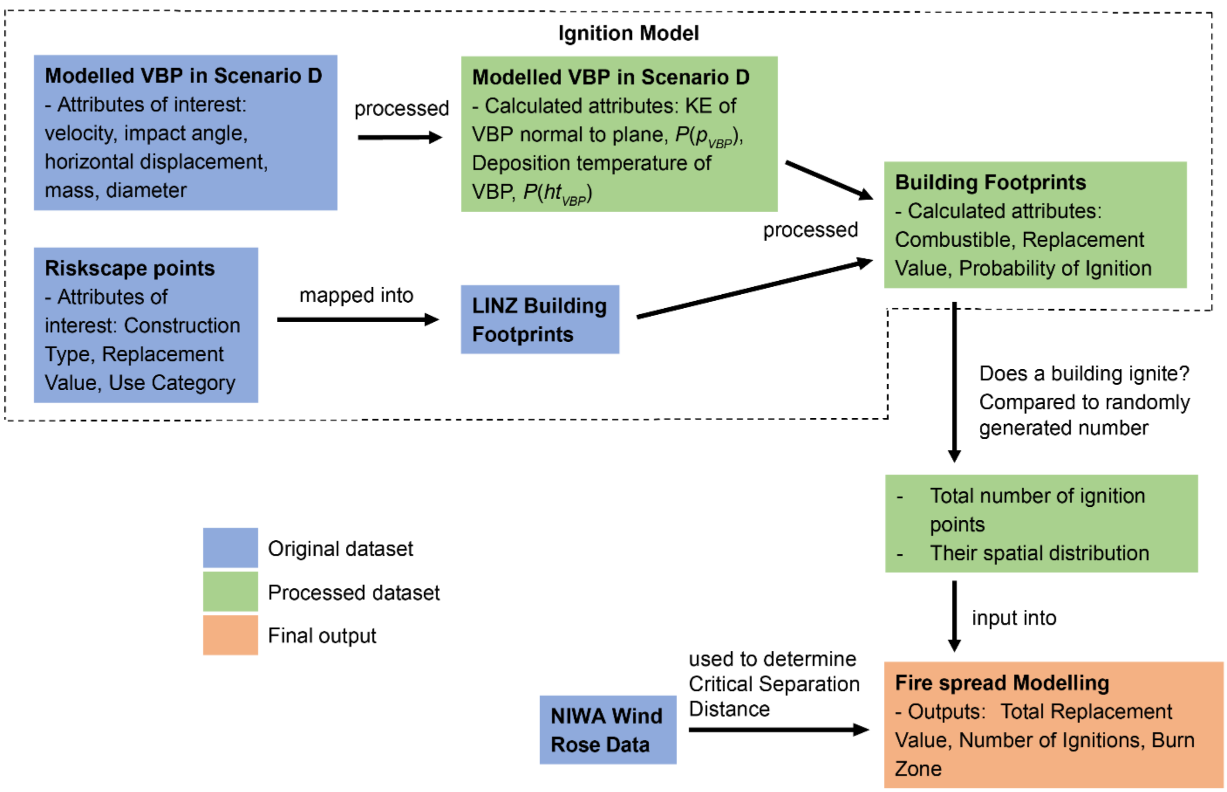

Figure 4. *Flowchart of how the FFVA framework was applied to the Auckland case study. The ignition model was run once to obtain VBP ignition data, while the fire spread model was run 50 times for each permutation of wind speed and direction to evaluate the effect of wind conditions on spread.*

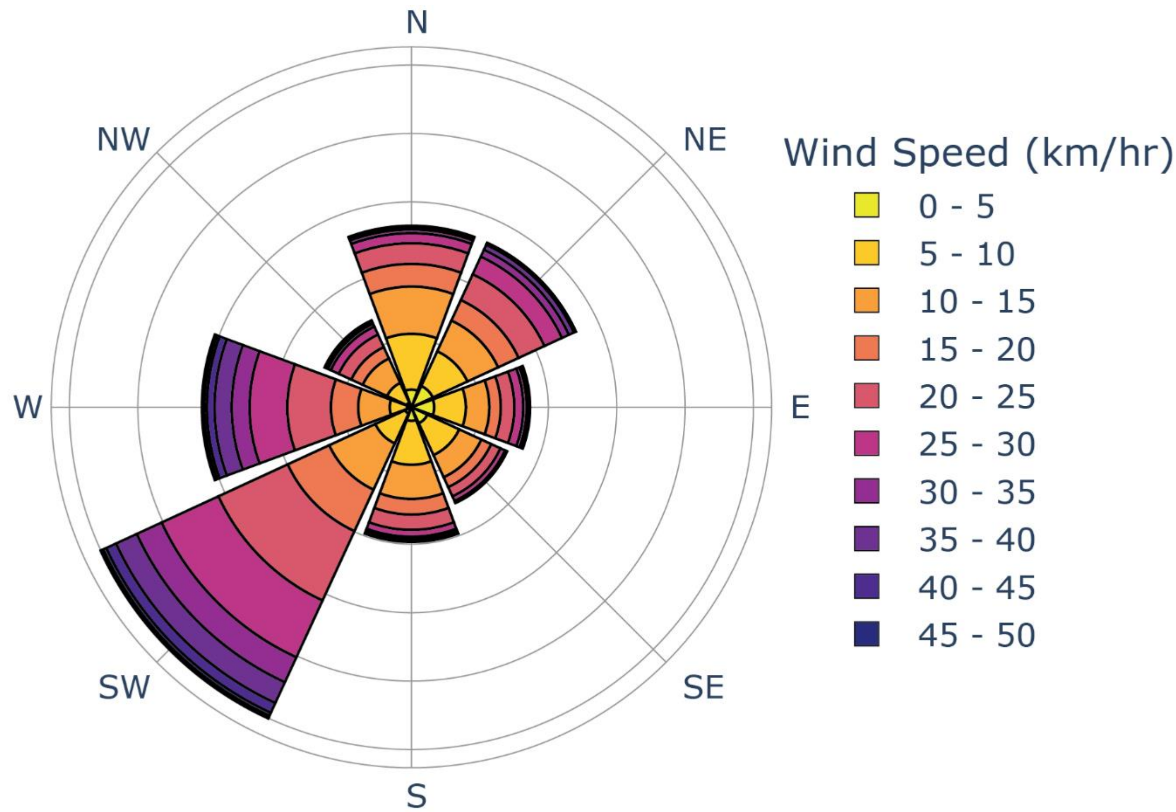

Figure 5. *Wind Rose data from Auckland Airport wind station. Average wind speeds are taken over the 10-minute period preceding each hour, from 1 January 1993 to 31 December 2002.*

3.3 Ignition model parameters

3.3.1 Calculating probability of perforation

We use the fragility curves developed by Williams et al. (2017) to calculate the probability of perforation for each building. These fragility curves estimate the probability of buildings exhibiting different states of damage as a function of the impact energy of the VBP landing on it. The fragility curves are presented using a three-tiered damage state system. Damage State 3 (DS3) represents the highest tier of roof damage possible from VBPs, in which the VBP has perforated the roof material, and therefore entered the building. At lower damages states (DS0-2) we assume that the VBP wedges/collides with the building but does not penetrate the walls or roof. Fragility functions developed by Williams et al. (2017) for VBP damage states are dependent on the velocity of each VBP normal to the building it impacts (V_n), which we calculate using the following:

$V_n = V_t * \cos(|\alpha - \gamma|) * \sin\theta$ (Equation 5)

Where: V_t is modelled impact velocity of the VBP, α is the roof pitch, γ is the impact angle of the VBP with respect to vertical, and θ is the angle between $V_t * \cos(|\alpha - \gamma|)$ and the roof plane, which accounts for varying building orientation with respect to the vent. In this work, we assumed a planar roof pitch of 27°, the average of Auckland residential properties contained within the RiskScape building database. θ is randomly sampled from a uniform distribution between 0 and 90° to account for differing orientations of the vent-facing roof plane.

We used the fragility curves from Williams et al. (2017) for 2x4 timber and reinforced concrete building cladding, which are the building materials for 98% of Auckland residential buildings in the RiskScape building database. The normal velocity of each VBP calculated in Equation 5 was used to determine the kinetic energy (KE) normal to the building:

$KE = \frac{1}{2} \times m \times {V_n}^2$ (Equation 6)

Where: *KE* is the kinetic energy of the VBP upon impact with the building (measured in Joules), *m* is the mass of the VBP and V_n is the component of velocity of the VBP normal to the plane of the building it impacts. Using the fragility curve and the derived KE, it is possible to determine the probability of each VBP perforating the building (Figure 6a).

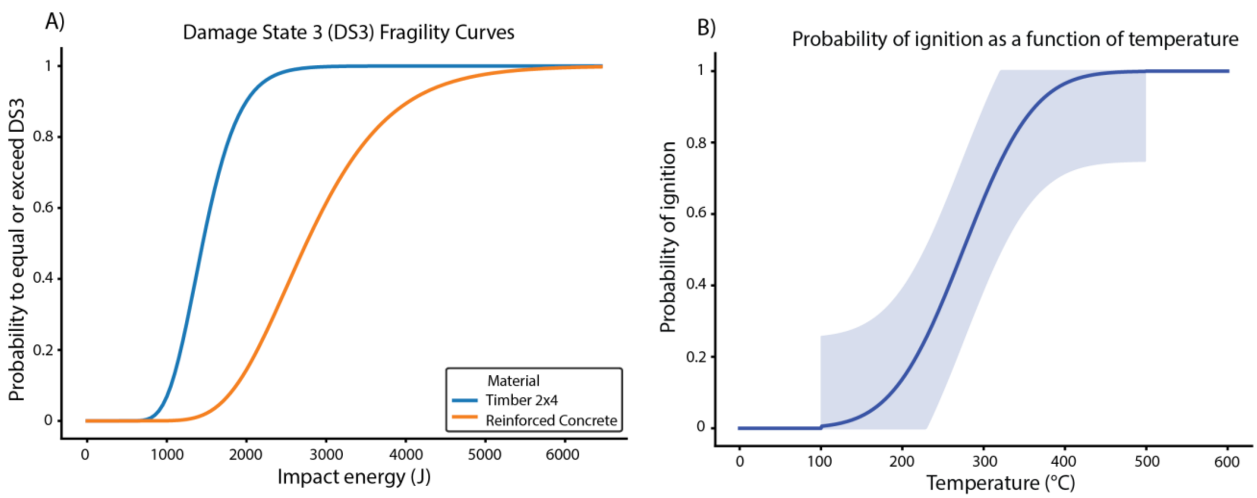

Figure 6. *Components of the ignition model: A) fragility curves for timber 2x4 and reinforced concrete building cladding materials. Increasing kinetic energy of the VBP results in a higher probability of roof perforation (after Williams et al., 2017), B) temperature vs. probability of ignition curve based on expert judgement of fire engineers. Uncertainty of ignition is based on a variety of conditions at temperatures between 100 and 500 °C reflected in the 0.25 error (light blue area extending from curve).*

3.3.2 Calculating probability of heat transfer

3.3.2.1 Estimated temperature for VBPs

VBP temperature upon impact is an important variable for ignition models as it will inform whether a given material the VBP lands on will catch fire. Thus, there are two considerations necessary for calculating the probability of heat transfer: 1) temperature of a ballistic upon impact with a building, and 2) probability of ignition of a material that comes into contact with a ballistic of a given temperature.

The deposition temperature of a VBP is dependent on the initial ejection temperature of the ballistic and its cooling rate as it travels through the air before impact. The model developed by Capaccioni and Cuccoli (2005) for ballistic transport of bombs in fire fountaining eruptions was the most appropriate analogy we could find. All VBPs in our scenario were binned into the same 3 clast sizes (-6, -7, and -8 ϕ), and we assumed a starting temperature (1026 °C) and cooling rates based on Figure 5 of Capaccioni and Cuccoli (2005).

3.3.2.2 Ignition model

The next step was to consider the probability that a material will ignite when in contact with a VBP of a given temperature. There have been no direct measurements of VBP ignition that we can use to inform our analysis. Indeed, the concept that a surface will ignite at a material-dependent critical temperature is itself an oversimplification of the complex phenomenon of ignition. The ignition is further complicated by the situation (orientation, surface finish, unexposed boundary condition) and environmental conditions (humidity, air movement). Due to the complex nature of ignition (see Babrauskas, 2003), we took a pragmatic approach, relying on ignition temperature data available in the literature over a range of time scales from seconds to months, and the expertise of a fire engineer (CF). The temperature-ignition probability curve (Figure 6b) assumes that above 500°C all buildings made of combustible material will ignite (i.e., timber; probability = 1). The 500°C was taken from autoignition data (230-530°C; Babrauskas, 2001) where ignition occurs without an ignition source present. The 50% chance of ignition at temperatures between 250 and 300 °C was taken from piloted ignition experiments (210-480°C; Babrauskas, 2001) where the ignition occurs in the presence of an ignition source (small flame or electric arc). Ignition was not considered possible for impact temperatures below 100 °C for buildings of any material (probability = 0) based on long-term exposure of wood for days to months (Babrauskas, 2003). Based on the above considerations, we used a normal distribution with a mean of 275 °C and a standard deviation of 68.75 °C (25% of the mean) to represent the temperature-ignition curve. A 25% probability error was allowed for all intermediate temperatures to reflect the uncertainty of ignition. Ignition probabilities were stochastically sampled from within this range using a uniform distribution to further account for uncertainty. This curve was applied to all timber buildings, based on the condition that all materials, including timber framing and building interiors, follow the same ignition probability curve.

3.3.3 Calculating probability of fuel availability

Different building compositions will have different susceptibility to ignition (i.e., a timber building is more susceptible to ignition than a reinforced concrete building). We account for this using the probability of available fuel parameter. Thus, to distinguish the fire load density (energy content of combustible materials per volume; Fontana et al., 2016) of timber from reinforced concrete houses, different values were set for *P(availability of fuel)*: 1 for timber and 0.5 for reinforced concrete, with all buildings treated as single component. This is in line with previous fire spread models and accounts for the importance of the interior and cladding of housing in fire spread even when the structural frame is not combustible; this assumes a combustible weatherboard cladding, common in NZ housing (Scheele et al., 2019). We do not account for vegetation adjacent to houses, which, due to their ease of ignition, can effectively expand the ignition-susceptible boundary of a building.

3.4 Auckland fire spread model

In this study, we used a fire spread model based on a burn zone model developed to aid in FFE risk analysis in Wellington, ANZ (Cousins et al., 2002, 2003; Scheele et al., 2019). This model, which operates according to the principles described in Section 2.3, was selected because of its transferability for use throughout ANZ and validation in an ANZ context by comparison to fire spread following the 1931 Hawke's Bay earthquake (Thomas et al., 2006). The model was applied in our study simply by substituting earthquake-related ignition locations for VBP-caused ignition locations. The fire spread model was run a total of 4,000 times: 50 times for each permutation of wind direction (8 directions) and CSD (10 values, derived from wind speed (Table 3)).

The model does not account for mitigation actions that might affect or inhibit the spread of fire started by VBP. Immediate mitigation and fire suppression in the event of an Auckland eruption may be challenging, as the city's evacuation policy enacts a 5 km exclusion zone around the vent site in the event of any eruption (Auckland Council, 2015). Access within this zone during an eruption would likely be subjected to considerable life safety risk analysis given the potential threats posed by an ongoing eruption. Understanding how fire spread can extend the threat outside of this 5 km zone acted as a prime driver for our study as it is key information that can support decision-making and preparedness.

4 Case study results

To compare the influence of fire spread and whether it has an important influence on potential emergency management and building losses, it is necessary to consider the area impacted and building loss that would likely occur when no fire is ignited and spread. To do this, we define a heavy damage zone (HDZ) based on the maximum area affected by VBPs for our scenario. This is an area likely to be subjected to heavy damage from a variety of different volcanic hazards (e.g., heavy tephra fall, earthquakes, deformation, edifice formation). It represents the maximum extent of VBP deposition modelled (a circular area of 0.89 km^2 centred on the vent, with radius 0.53 km), though not all of the buildings within this area were impacted by VBPs. The extent of this area is similar to previous work that identified areas of assumed total destruction in the AVF (Houghton et al., 2006; Németh et al., 2012; Deligne et al., 2017a,b). In our model of DEVORA Scenario D, 574 of the 976 buildings within the HDZ (59%) were affected by at least one VBP, and 285 buildings within the HDZ (29%) have an ignition probability greater than 0 (i.e., availability of fuel and heat transfer allow for ignition). There is a clear attenuation of ignition probability with distance from the vent (Figure 7), reflecting the attenuation of VBP deposition with distance from vent as well as cooling of the VBPs during transit reducing the probability of heat transfer.

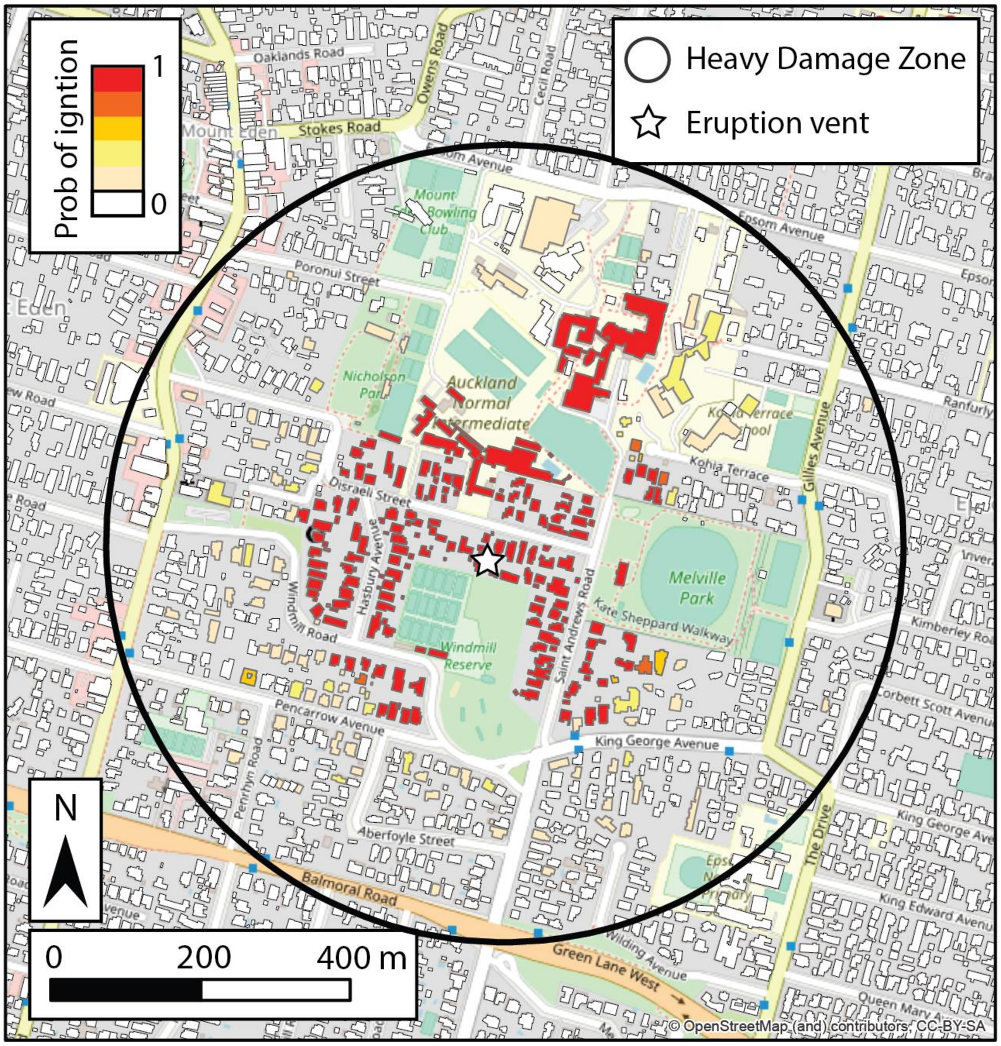

Figure 7. *Probability of ignition of buildings in DEVORA Scenario D. Blue circle represents VBP damage area, i.e., the maximum extent of VBP deposition modelled, referred to here as the Heavy Damage Zone (HDZ).*

4.1 Fire spread modelling results

Fire spread modelling results are described in terms of the different permutations of wind direction and CSD (since CSD is directly related to wind speed and the model determines burn zone using CSD). For example, permutation N 13m represents a northerly wind (blowing north to south) with a 13 m CSD, reflecting wind speeds between 5 and 15 km/hr (Table 3).

To evaluate whether FFVA is an important hazard in need of risk management consideration we compare damage area and building loss from the HDZ (the primary volcanic hazard) to that from the fire spread burn zones produced, focusing on additional damage and loss to that seen in the HDZ. The HDZ in Scenario

D is 0.89 km^2 and has residential building loss exposure of approximately NZ$0.69 billion, assuming all buildings within it are a total loss due to the high exposure to a variety of volcanic hazards.

In our model results, damage exceeding this area and building loss value occurs due to a combination of wind direction and speed, and available buildings, with a CSD of 33 m or greater leading to total burn zone areas >1 km^2 and damage values over $NZ0.7 billion (Figure 8). For the eruption scenario and location considered here, FFVA is unlikely to spread significantly beyond the HDZ or cause building loss values greater than those in the HDZ in conditions where the CSD is under 28 m (with the model caveat that fire spread through vegetation is not considered). The critical CSD of 33 m or more results from wind speeds greater than 40 km/h. In Auckland, these conditions occurred 2.61% of the time over the past 10 years. Based on seasonal wind patterns, these conditions are most common between September-November and between June-August.

It is also evident that at CSD 33 m+, not only does the burn zone area and residential losses increase, but the fire spread model results become highly uncertain. For example, a wind blowing from the NW and a CSD of 45 m results in a burn zone that can vary four-fold and residential losses vary approximately five-fold. The distributions also change from largely normally distributed with little to no skewing for CSD 18-28 m to more varied at CSD 33 m+ distributions, with highly skewed uni-modal (e.g., N 42) and bi-modal distributions (e.g., E 45, NW 45) becoming evident. The results for burn area and residential building losses exhibit similar ranges and distributions within those ranges, suggesting a relatively uniformly distributed building stock.

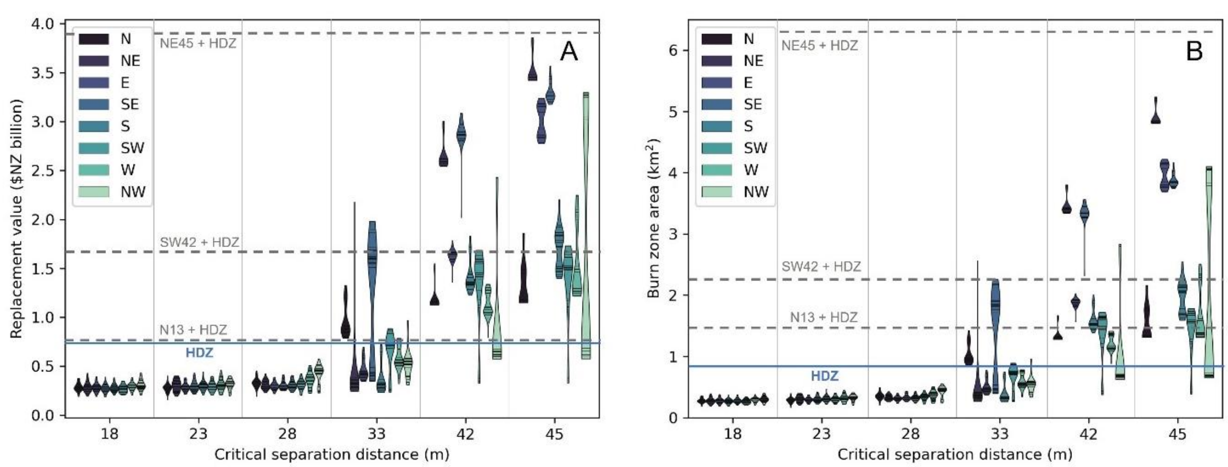

Figure 8. *Violinplot of critical separation distance (CSD) with A) Residential building losses, and B) Burn zone area. For each CSD, eight individual results are shown, representing each wind speed bin. The spread in area or loss values for each violin represents the range of values obtained from the 50 simulations for*

each wind direction and CSD permutation. NE45, SW42, and N13 refer to key wind permutations we explore in section 4.2.

In addition to CSD, wind direction can play a large role in controlling the burn zone size and amount of damage by directing the fire towards more built areas, which promotes fire spread. In Scenario D, wind direction from the north and southeast has the highest potential for the burn zone to exceed the HDZ at the lowest CSD. A CSD of 33 m with wind directions from the N and SE can produce mean burn zones of 1 and 1.4 km^2 (NZ$0.97 billion and NZ$1.2 billion replacement value), respectively. Meanwhile, at the highest CSD (45 m), a northeasterly wind produces the largest mean and maximum burn zone of 4.9 km^2 and 5.2 km^2 (NZ$3.5 billion, NZ$3.9 billion replacement value), respectively (Figure 9); this is around 1 km^2 (and NZ$0.2billion) greater than those sustained by any other wind direction and speed.

The third key factor affecting burn zone area and building losses is the distribution of the buildings themselves. Scenario D is located in an area with a number of recreational areas, seen as irregularly shaped space with no buildings on Figure 7. Linear areas with no buildings are typically roads and large irregular empty spaces between buildings are frequently parks. As we only simulate fire spread between buildings, these no-building areas act to limit fire spread; thus, a wind blowing from the west needs a larger CSD than one blowing from the east in order to affect a similar number of buildings. This can be seen in Figure 8, where winds from the NE through SE typically have larger burn zones and building losses than those from other directions (because of the relatively higher density of buildings and the ability for fire to spread from building to building). This is especially prominent with faster wind speeds.

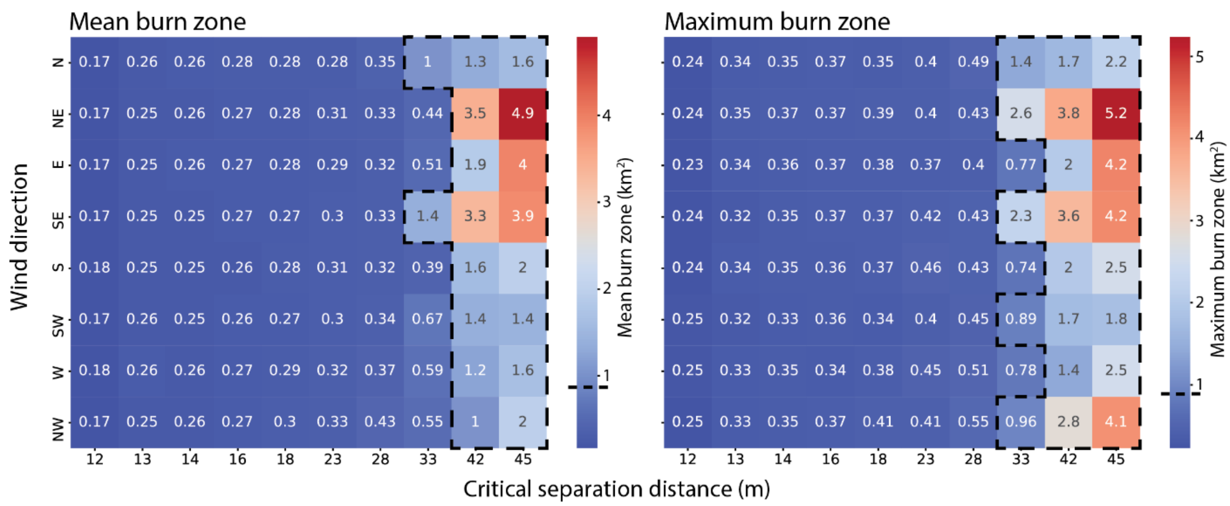

Figure 9. *Heatmaps of the mean and maximum burn zones for each permutation of wind direction and critical separation distance. Black line on the scale bar represents the HDZ area (0.89 km^2). Boxes contained by black dashed lines represent permutations that produce a burn zone equal to or greater than the HDZ area.*

4.2 Key wind permutations

We highlight three wind permutations that represent likely and damaging FFVA based on maximum burn zone (Figures 9 and 10): i) the most common Auckland wind pattern (N 13m) (Fig. 5); ii) the major fire spread conditions permutation (SW 42m), which was based on the most commonly occurring wind pattern to result in a burn area that would extend beyond the HDZ; and iii) the maximum credible permutation (NE 45m), which resulted in the largest mean and maximum burn area. Based on the 10-year wind history, these wind directions occur in Auckland at 7.4, 0.25, and 0.03% frequency, respectively (with some seasonal variance). In calculating the value of damage caused by FFVA, we considered values in in the RiskScape database (NZD c. 2015), with damage only accounting for building structures (not contents or adjacent objects like pathways) (Table 4).

Table 4: Summary results of key case study wind permutations. Damage in the HDZ was considered to equal the full replacement cost of buildings in that area.

	Heavy damage zone (0.89 km^2)	Most common wind pattern: N 13m (Mean values)	Major fire spread conditions: SW 42m (Mean values)	Maximum credible permutation: NE 45m (maximum values)
Frequency of wind conditions	-	7.4%	0.25%	0.03%
Burn zone (km^2)	-	0.25	1.4	5.2
Replacement cost in billion NZ dollars*	0.69	0.34	1.4	3.9
Replacement cost outside the HDZ in billion NZD*	0	0.0072	0.93	3.4

*In the heavy damage zone, the replacement cost considers full loss of all buildings within this area. In fire spread permutations, replacement cost considers full loss of all burned buildings only. Building values in NZD c. 2015 as presented in the RiskScape building database.

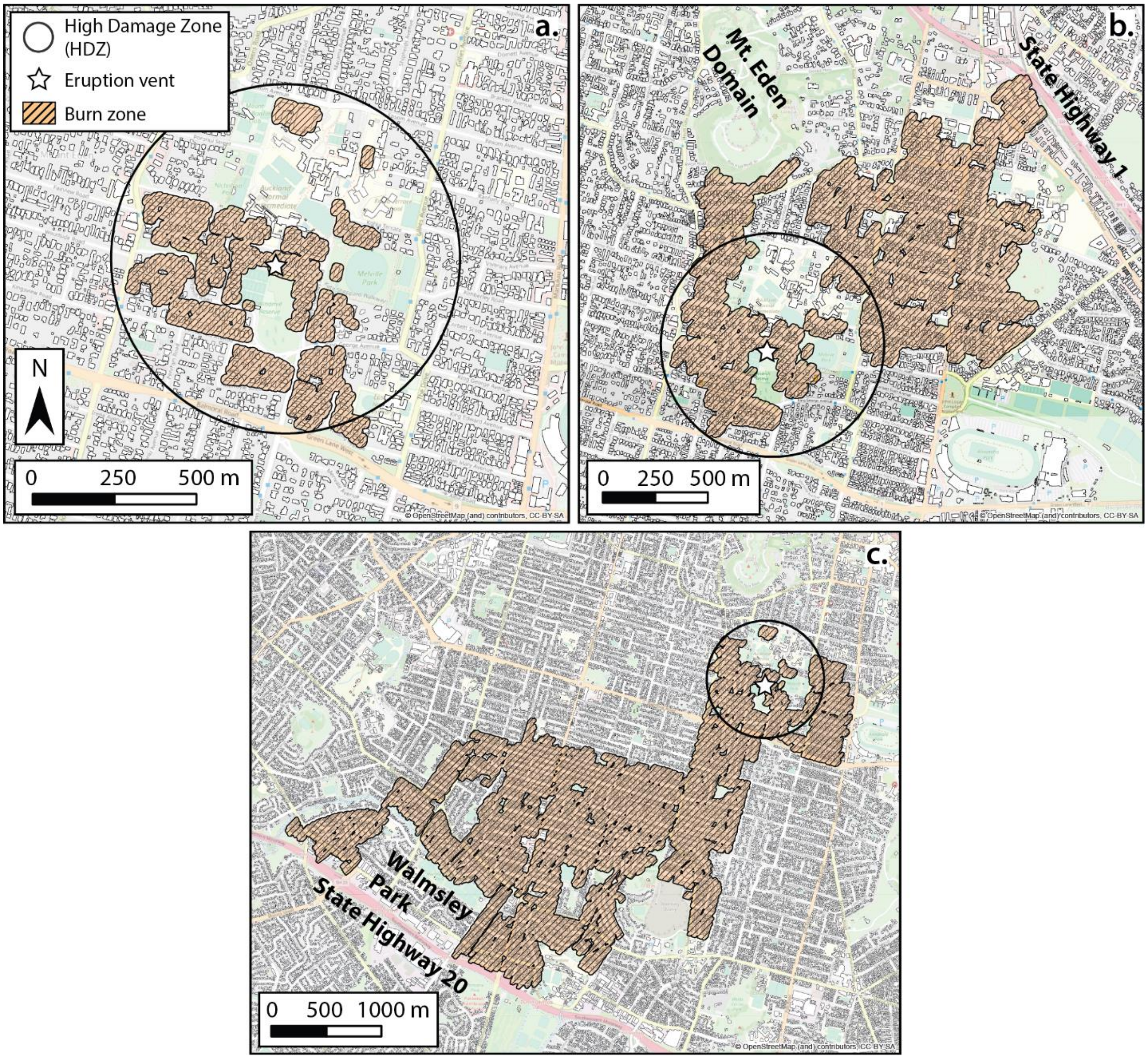

Figure 10. *Burn zone maps showing area affected by FFVA in wind permutations representing the: a) most common Auckland wind pattern (N 13m), b) most common wind pattern to cause major damage (SW 42m), c) maximum credible damaging permutation (NE 45m).*

4.2.1 Likely fire spread conditions (N 13m)

The most common wind pattern in Auckland is a 5-15 km/h northerly wind (7.5% occurrence), which results in a CSD of 13 m and a burn zone area of 0.25 km^2 (Figure 10a). In this case, most of the burn zone is within the HDZ, with only 2.4% (0.006 km^2) extending beyond the HDZ boundary. In this permutation, the low CSD means that building distance and small roads contain the fire spread. The burn zone footprint in this permutation includes approximately NZ $0.34 billion of residential property, but only NZ $0.0072 billion in replacement value located within the burn zone is beyond the HDZ.

4.2.2 Major fire spread conditions (SW 42m)

The most likely wind permutation to cause major damage (damage extending beyond the 0.89 km^2 HDZ) is a 45-49.9 km/h southwesterly wind (0.25% occurrence), resulting in a CSD of 42 m. This permutation affects an area of 1.4 km^2, approximately 60% greater than the HDZ (Figure 10b). The burn zone for this permutation includes NZ $1.4 billion in residential buildings, with approximately 71% falling outside the boundary of the HDZ. This indicates that a wind permutation with these conditions would likely cause substantial residential building losses (NZ $1 billion) beyond the HDZ. Fire spread in this permutation is stopped by elements that create insurmountable distance between buildings for spread, including State Highway 1 east of Mt. Eden suburb and Mt. Eden domain, which is a vegetated park at the northwest of the burn zone.

4.2.3 Maximum credible fire spread conditions (NE 45m)

The most damaging FFVA permutation modelled in this study results from a 50+ km/h northeasterly wind (0.03% occurrence), with a CSD of 45 m. In this permutation, the area of the burn zone (5.2 km^2) is six times greater than the HDZ (Figure 10c), and the value of the residential buildings located within the burn zone is NZ $3.9 billion, more than five times greater than the value located within the HDZ. Strong wind conditions such as these facilitate considerable fire spread and additional damage (NZ $3.4 billion; 87% of fire-damaged residential building value) beyond the HDZ. Walsmley Park and State Highway 20 at the south of the burn zone act as fire breaks within the model, which prevent even further fire spread in this permutation.

5 Discussion

Our application of FFVA shows that it is a non-trivial threat that warrants consideration within volcanic hazard and risk assessments and emergency management planning. Our results show that there may be considerable additional impacts above those directly associated with other volcanic hazards. However, the exact scale of this is dependent on a number of key factors. Firstly, the CSD, wind direction, and density of fuel sources (e.g., houses) influences the extent of fire spread. In our case study, at CSD below 33 m, the burn area is small and rarely extends beyond the HDZ damage (e.g., permutation N 13m), regardless of wind direction (Figure 8). At higher CSD values (CSD 33 and above), the damage area and value are much more variable based on wind direction. This may be because, in contrast to low CSD permutations where fire is unlikely to spread based on the location and density of buildings in the immediate vicinity of our HDZ and Scenario D's hypothetical vent location, in high CSD permutations, where the building distance in our case study chosen location supports fire spread, the direction and extent of spread is then more dependent on the layout of buildings and presence of firebreaks. An additional important factor controlling fire spread is the presence of link bridges—individual timber buildings that serve to connect larger clusters of ignitable buildings. Whether these link bridges are present and whether they ignite can have a significant impact on the total damage in high CSD permutations. The importance of building density, firebreaks, and link bridges also highlights the sensitivity of our model to the vent location in the setting of a volcanic field—the presence and extent of these variables can be highly dependent on where across a large area the eruption occurs.

The two wind permutations producing high damage presented in this paper (SW 42m and NE 45m) highlight the importance of firebreaks in preventing spread but also highlight a limitation of the fire spread model. In both these permutations, the spread of FFVA was halted by the presence of gaps between buildings. State Highways 1 and 20 act as a true firebreak in each permutation, creating gaps between buildings too great for the fire to spread. At low CSD values (CSD < 33), smaller local roads can sometimes be sufficient to act as firebreaks, hence the lack of significant spread in low wind conditions. By contrast, Mt. Eden Domain in the SW 42m permutation and Walmsley Park in the NE 45m permutation may not be true firebreaks, but rather a representation of the model's inability to capture fire spread through local parks and recreation areas. Both are highly vegetated, and it is possible that fire could spread through them under the right conditions. This means that our fire spread model may underestimate the size of the burn zone in similar permutations. This is an important improvement to be made to this model in the future.

Existing evacuation policy in Auckland is to create a two-part exclusion zone based on expected hazards and damage to critical infrastructure, with an estimated primary exclusion zone up to 3 km from the vent and secondary exclusion zone between 3 and 5 km from the vent (Auckland Council, 2015). Based on this policy, none of our fire burn zones would extend beyond a 5 km anticipated evacuation zone. In the case of the NE 45 m permutation, the fire spread is stopped only by the placement of the State Highway 20. The Mangere Inlet is approximately 5 km from the vent location, meaning that if the fire did manage to spread across State Highway 20, it would be prevented from further spread upon reaching the coast. Thus, in this specific permutation, fire would be unlikely to be able to extend into areas that would not have already been evacuated. However, we have assumed a constant wind in our analysis. If this were to change during the course of the fire spread (e.g., before the fire reaches State Highway 20), it may be possible for fire to reach areas that would not have been evacuated. Likewise, we have ignored the effects of vegetation, topography, and other volcanic hazards across all permutations in this work, which could mean that fire would extend farther than we have modelled. Finally, we have simulated fire spread for one specific scenario and location, and one specific building stock and distribution; given we do not know where the next vent will be, other areas of Auckland where an eruption could occur may have different susceptibility for fire spread. Thus, the potential for fire spread beyond evacuation zones designed for volcanic hazards may be an important consideration with regards to human safety and evacuation.

The results of the case study demonstrate clearly that FFVA can significantly increase the damage caused by eruption, regardless of whether the fire spreads beyond the zone directly affected by volcanic hazards. This is seen clearly in the maximum credible case (Figure 10c), where the fire spread covers an area over six times that of the HDZ and causes more than five times the monetary loss represented by the HDZ alone. However, even in the most common wind permutation (Figure 10a), where the burn zone covers an area smaller than the HDZ (and only a small portion of the damage occurs beyond the HDZ), FFVA would likely result in some amount of damage additional to that caused by other hazards and could result in greater losses to buildings within the HDZ that were not fully destroyed by other hazards (that are assumed as total loss in our study).

We have assumed that fires can spread unchecked based on the assumption that firefighting capability during or following an eruption may be severely constrained. There will likely be access difficulty due to restrictions for life safety considerations related to an ongoing eruption, and due to damaged ground transportation networks (Deligne et al., 2017a; Blake et al., 2017). Water shortages have also been experienced following eruptions due to damage to water infrastructure and overuse from clean-up activities (Stewart et al., 2006; Wilson et al., 2012; Wilson et al., 2014; Hayes et al., 2015). Thus, fire suppression may be limited in the event of fire during an active eruption. Further investigation of potential firefighting decision-making during and following volcanic eruptions may help identify tailored strategies for fire suppression and may vary depending on eruptive vent location and style, local government and emergency management structures.

Differentiating between causes of damage to a building is important for both insurance and recovery purposes. Some insurance policies may pay out for fire damage, but not for volcanic eruption damage (or vice versa) (Blong et al., 2017). Thus, insurers and/or insureds may not have a true appreciation of their loss exposure. Recovery processes may also be complicated by fire damage and the necessary clean-up and disposal requirements. For example, the waste produced by fire damage may require specialized removal in order to manage public health hazards that it can produce (Brown et al., 2011; Hayes et al., 2021).

5.1 Future work

Due to the limited research undertaken assessing the potential for FFVA, many of the model parameters and assumptions require validation. In addition to better modelling of fire spread through vegetated or topographically variable areas, our models could benefit from more empirical and historical validation. Our fire spread model has been previously validated with respect to FFE using the 1931 Hawke's Bay earthquake but needs comparison to real FFVA scenarios (e.g., the 2021 Cumbre Vieja eruption resulted in lava flow-ignited fires, which could be used to validate the fire spread model; Longpré 2021). Retrospective fire spread modelling for historic eruptions where fire spread is known to have occurred may be beneficial to test and evaluate specific modelling assumptions and their applicability in a volcanic eruption setting. Fire spread is controlled by wind conditions but also the availability of fuel, which will vary by building type, vegetation type, moisture content of the fuel, geographic distribution and the presence or absence of firebreaks such as roads. Thus, validating with as many previous examples of FFVA as possible will help to capture some of the uncertainty in our assumptions and modelling. Use and availability of more precise data is also likely to produce better results. For example, VBP temperature and cooling rates more precise to the modelled eruption and more precise data on the building material of impacted buildings (i.e., "availability of fuel") and how they respond to different volcanic hazards (i.e., "probability of ignition").

Based on the results of our case study, it is evident that FFVA is an issue worthy of further investigation, both in Auckland and at active volcanoes more broadly. In particular, the susceptibility for fire spread will probably be heterogeneous across Auckland due to differing building typologies and building densities as well as topography and vegetation. This complication may be even greater in localities with more variable building typologies. Here, we assumed residential building stock while Auckland has commercial, industrial, and residential buildings, among others, that likely vary in fuel loads and combustibility. Thus, we suggest that more in-depth probabilistic modelling that accounts for varying eruption location, style and timing, inclusion of additional building typologies and fuel sources, and inclusion of other primary volcanic hazards would be beneficial to further quantify fire spread susceptibility and risk following volcanic eruptions.

In this work we have modelled VBP-induced fire ignition in isolation of other hazards that are likely to be occurring before, during and after the VBPs impact buildings. How these hazards interact and influence the probability of ignition requires more consideration. Changes to the built environment due to other hazards such as PDC or lava flows could actually reduce the ability of FFVA to spread by removing available buildings (fuel) and increasing gaps between flammable objects. Lava flows can even act as firebreaks by providing non-flammable obstacles for the fire (Meredith et al., 2022). They could also reduce the number of buildings available to be impacted and ignited by VBP. Alternately, the potential for fire spread could be increased by kinetic forces damaging buildings and exposing flammable materials, allowing them to more readily catch fire. PDCs and lava flows could strip vegetation from the landscape, removing material that could be ignited, potentially turning previously vegetated areas into effective firebreaks. By contrast, PDCs could potentially dry/char vegetation in wet conditions, increasing their ability to be ignited (Jenkins et al., 2013). Tephra fall has also been shown to decrease the probability of roof perforation (Williams et al., 2017), which would decrease the probability of ignition of building interiors (though potentially increasing the probability of building exteriors). Of course, all of these additional hazards also have the potential to ignite fires, possibly increasing the overall probability of FFVA. Ignition and fire spread modelling of other hazards such as lava flows, fire fountaining, and PDCs, as well as more complex multi-hazard models would be a valuable extension of the findings of this study.

A variety of improvements can be made in future FFVA modelling to provide more realistic and complex results. Future models should incorporate vegetation and topography, two factors unaccounted for at present that certainly affect fire spread. Spatio-temporal evolution of fire ignition and spread is an important component of fire risk modelling. For example, we have assumed all VBPs hit contemporaneously, and all ignitions are subjected to the same wind conditions. In reality, there will be waxing and waning of when VBP are ejected during the eruption and environmental conditions such as wind and precipitation are likely to change, particularly over relatively long-lived eruptions. The timing of VBP impacts may mean that ignitions occur over an elongated period of time, but we have largely ignored this effect in our initial assessment for simplicity. However, the timing of ignitions and changes in environmental conditions are likely to be important elements affecting the likelihood and scale of fire spread.

6 Conclusions

FFVA is an important hazard that is rarely considered within volcanic hazard and risk assessments. Previous eruptions have demonstrated the additive effect fire can have on the societal impacts of volcanic eruptions. In this paper, we propose a modelling framework that facilitates the integration of FFVA into volcanic risk assessment. The framework is underpinned by a fault tree that allows one to logically layout potential fire ignition sources for volcanic eruptions. Probabilities and uncertainty can then be transparently tracked and propagated through the analysis. We demonstrated the use of this framework by assessing potential fire spread from a volcanic eruption scenario in the AVF using VBPs as an ignition source. This application has identified important areas of future consideration about post-eruption fire risk in Auckland and more broadly. We found that losses may be increased above levels that would have been expected from the other volcanic hazards alone, indicating the compounding effect fire may have in future eruptions. While the models and framework presented here provide a solid starting point in assessing FFVA risk, they would benefit from additional research in a number of areas, including probabilistic modelling to better capture the potential for FFVA across multiple eruption scenarios, environmental conditions, and in the case of Auckland and other volcanic fields, multiple potential eruption locations and thus building typologies and distributions. Incorporating multi-hazard interactions between hazards over time and how that may contribute to FFVA is an additional future avenue for research, as is validating the approach and modelling with past examples of FFVA. We believe that this work highlights the importance of accounting for FFVA in volcanic risk assessment and emergency management and hope to see increased attention to this this topic in the future.

Acknowledgements

JYQ was supported by Nanyang Technological University CN Yang Scholars Program. GAL and SFJ acknowledge funding from AXA and Singapore National Research Foundation (NRF2018NRF-NSFC003ES-010). JLH acknowledges funding from AXA. JLH was supported by the New Zealand Ministry of Business, Innovation and Employment (MBIE) through Hazards and Risk Management programme (Strategic Science Investment Fund, contract C05X1702). This research was supported by the Earth Observatory of Singapore via its funding from the National Research Foundation Singapore and the Singapore Ministry of Education under the Research Centres of Excellence initiative. EOS contribution number 456.

Author Contributions

SFJ conceived the study, with methodology developed by JYQ, JLH, RHF, SFJ, and TMW. JYQ, JLH, and RHF performed the investigation and analyses, with JYQ supervised by JLH, RHF, SFJ, and TMW. GAL led the writing, alongside JYQ, JLH and RHF, and GAL organized the final manuscript. FS, BL, CF provided expert advice on the fire spread models and ignition probabilities. All authors reviewed and edited the manuscript.

Data Availability

Data used in this study are located in the DR-NTU (Data) repository at https://researchdata.ntu.edu.sg/privateurl.xhtml?token=0ca57b99-db85-4453-b65a-65e5dcef2c8e.

References

Ainsworth, A., Boone Kauffman, J., 2009. Response of native Hawaiian woody species to lava-ignited wildfires in tropical forests and shrublands, in: Van der Valk, A.G. (Ed.), Forest Ecology: Recent Advances in Plant Ecology. Springer Netherlands, Dordrecht, pp. 197–209. https://doi.org/10.1007/978-90-481-2795-5_15

Alvarado, G.E., Soto, G.J., Schmincke, H.-U., Bolge, L.L., Sumita, M., 2006. The 1968 andesitic lateral blast eruption at Arenal volcano, Costa Rica. Journal of Volcanology and Geothermal Research, Arenal Volcano, Costa Rica 157, 9–33. https://doi.org/10.1016/j.jvolgeores.2006.03.035

Ang, P.S., Bebbington, M.S., Lindsay, J.M., Jenkins, S.F., 2020. From eruption scenarios to probabilistic volcanic hazard analysis: An example of the Auckland Volcanic Field, New Zealand. Journal of Volcanology and Geothermal Research 397, 106871. https://doi.org/10.1016/j.jvolgeores.2020.106871

Auckland Council, 2015. Auckland Volcanic Field Contingency Plan. Auckland Emergency Management.

Babrauskas, V., 2003. Ignition Handbook. Fire Science Publishers, Issaquah, WA.

Babrauskas, V., 2001. Ignition of Wood: A Review of the State of the Art. Interscience Communications Ltd., London, pp. 71–88.

Baxter, P.J., 1990. Medical effects of volcanic eruptions: I. Main causes of death and injury. Bull Volcanol 52, 532–544. https://doi.org/10.1007/BF00301534

Baxter, P.J., Boyle, R., Cole, P., Neri, A., Spence, R., Zuccaro, G., 2005. The impacts of pyroclastic surges on buildings at the eruption of the Soufrière Hills volcano, Montserrat. Bull Volcanol 67, 292–313. https://doi.org/10.1007/s00445-004-0365-7

Bebbington, M.S., Cronin, S.J., 2011. Spatio-temporal hazard estimation in the Auckland Volcanic Field, New Zealand, with a new event-order model. Bull Volcanol 73, 55–72. https://doi.org/10.1007/s00445-010-0403-6

Blake, D.M., Deligne, N.I., Wilson, T.M., Lindsay, J.M., Woods, R., 2017. Investigating the consequences of urban volcanism using a scenario approach II: Insights into transportation network damage and functionality. Journal of Volcanology and Geothermal Research 340, 92–116. https://doi.org/10.1016/j.jvolgeores.2017.04.010

Blong, R., Tillyard, C., Attard, G., 2017. Insurance and a Volcanic Crisis—A Tale of One (Big) Eruption, Two Insurers, and Innumerable Insureds, in: Fearnley, C.J., Bird, D.K., Haynes, K., McGuire, W.J., Jolly, G.

(Eds.), Observing the Volcano World: Volcano Crisis Communication, Advances in Volcanology. Springer International Publishing, Cham, pp. 585–599. https://doi.org/10.1007/11157_2016_42

Blong, R.J., 1984. A Sourcebook on the Effects of Eruptions. Academic Press, Sydney.

Brown, C., Milke, M., Seville, E., 2011. Disaster waste management: A review article. Waste Management 31, 1085–1098. https://doi.org/10.1016/j.wasman.2011.01.027

Brown, R.J., D. M. Andrews, G., 2015. Chapter 36 - Deposits of Pyroclastic Density Currents, in: Sigurdsson, H. (Ed.), The Encyclopedia of Volcanoes (Second Edition). Academic Press, Amsterdam, pp. 631–648. https://doi.org/10.1016/B978-0-12-385938-9.00036-5

Capaccioni, B., Cuccoli, F., 2005. Spatter and welded air fall deposits generated by fire-fountaining eruptions: Cooling of pyroclasts during transport and deposition. Journal of Volcanology and Geothermal Research 145, 263–280. https://doi.org/10.1016/j.jvolgeores.2005.02.001

Cicione, A., Walls, R., Sander, Z., Flores, N., Narayanan, V., Stevens, S., Rush, D., 2021. The Effect of Separation Distance Between Informal Dwellings on Fire Spread Rates Based on Experimental Data and Analytical Equations. Fire Technol 57, 873–909. https://doi.org/10.1007/s10694-020-01023-8

Coar, M., Sarreshtehdari, A., Garlock, M., Elhami Khorasani, N., 2021. Methodology and challenges of fire following earthquake analysis: an urban community study considering water and transportation networks. Nat Hazards 109, 1–31. https://doi.org/10.1007/s11069-021-04795-6

Cousins, J., Heron, D., Mazzoni, S., Thomas, G., Lloydd, D., 2002. Estimating Risks from Fire Following Earthquake (Client report No. 2002/60). GNS Science, Lower Hutt (NZ).

Cousins, J., Thomas, G.C., Heron, D.W., Mazzoni, S., Lloydd, D., 2003. Modelling the Spread of Post-earthquake Fire. New Zealand Society for Earthquake Engineering, University of Canterbury, Christchurch, p. 8.

Crawford, M.H., Crowley, K., Potter, S.H., Saunders, W.S.A., Johnston, D.M., 2018. Risk modelling as a tool to support natural hazard risk management in New Zealand local government. International Journal of Disaster Risk Reduction 28, 610–619. https://doi.org/10.1016/j.ijdrr.2018.01.011

Deligne, N.I., Fitzgerald, R.H., Blake, D.M., Davies, A.J., Hayes, J.L., Stewart, C., Wilson, G., Wilson, T.M., Castelino, R., Kennedy, B.M., Muspratt, S., Woods, R., 2017a. Investigating the consequences of urban volcanism using a scenario approach I: Development and application of a hypothetical eruption in the Auckland Volcanic Field, New Zealand. Journal of Volcanology and Geothermal Research 336, 192–208. https://doi.org/10.1016/j.jvolgeores.2017.02.023

Deligne, N.I., Horspool, N., Canessa, S., Matcham, I., Williams, G.T., Wilson, G., Wilson, T.M., 2017b. Evaluating the impacts of volcanic eruptions using RiskScape. Journal of Applied Volcanology 6, 18. https://doi.org/10.1186/s13617-017-0069-2

Fontana, M., Kohler, J., Fischer, K., De Sanctis, G., 2016. Fire Load Density, in: Hurley, M.J., Gottuk, D., Hall, J.R., Harada, K., Kuligowski, E., Puchovsky, M., Torero, J., Watts, J.M., Wieczorek, C. (Eds.), SFPE Handbook of Fire Protection Engineering. Springer New York, New York, NY, pp. 1131–1142. https://doi.org/10.1007/978-1-4939-2565-0_35

Geist, D.J., Harpp, K.S., Naumann, T.R., Poland, M., Chadwick, W.W., Hall, M., Rader, E., 2008. The 2005 eruption of Sierra Negra volcano, Galápagos, Ecuador. Bull Volcanol 70, 655–673. https://doi.org/10.1007/s00445-007-0160-3

Genareau, K., Gharghabi, P., Gafford, J., Mazzola, M., 2017. The Elusive Evidence of Volcanic Lightning. Sci Rep 7, 15508. https://doi.org/10.1038/s41598-017-15643-8

Genareau, K., Wardman, J.B., Wilson, T.M., McNutt, S.R., Izbekov, P., 2015. Lightning-induced volcanic spherules. Geology 43, 319–322. https://doi.org/10.1130/G36255.1

Gernay, T., Khorasani, N.E., 2019. Resilience of the Built Environment to Fire and Fire-Following-Earthquake, in: Noroozinejad Farsangi, E., Takewaki, I., Yang, T.Y., Astaneh-Asl, A., Gardoni, P. (Eds.), Resilient Structures and Infrastructure. Springer, Singapore, pp. 417–449. https://doi.org/10.1007/978-981-13-7446-3_16

Gordon, K.D., Cole, J.W., Rosenberg, M.D., Johnston, D.M., 2005. Effects of Volcanic Ash on Computers and Electronic Equipment. Nat Hazards 34, 231–262. https://doi.org/10.1007/s11069-004-1514-1

Harris, A.J.L., 2015. Chapter 2 - Basaltic Lava Flow Hazard, in: Shroder, J.F., Papale, P. (Eds.), Volcanic Hazards, Risks and Disasters. Elsevier, Boston, pp. 17–46. https://doi.org/10.1016/B978-0-12-396453-3.00002-2

Hayes, H., Josh L., Tsang, S.W., Fitzgerald, R.H., Blake, D.M., Deligne, N.I., Doherty, A., Hopkins, J.L., Hurst, A.W., Le Corvec, N., Leonard, G.S., Lindsay, J.M., Miller, C.A., Nemeth, K., Smid, E., White, J.D.L., Wilson, T.M., 2018. The DEVORA scenarios: multi-hazard eruption scenarios for the Auckland Volcanic Field (GNS Science report No. 2018/29). GNS Science, Lower Hutt, NZ.

Hayes, J., Wilson, T.M., Deligne, N.I., Cole, J., Hughes, M., 2017. A model to assess tephra clean-up requirements in urban environments. Journal of Applied Volcanology 6, 1. https://doi.org/10.1186/s13617-016-0052-3

Hayes, J.L., Wilson, T.M., Brown, C., Deligne, N.I., Leonard, G.S., Cole, J., 2021. Assessing urban disaster waste management requirements after volcanic eruptions. International Journal of Disaster Risk Reduction 52, 101935. https://doi.org/10.1016/j.ijdrr.2020.101935

Hayes, J.L., Wilson, T.M., Deligne, N.I., Lindsay, J.M., Leonard, G.S., Tsang, S.W.R., Fitzgerald, R.H., 2020. Developing a suite of multi-hazard volcanic eruption scenarios using an interdisciplinary approach. Journal of Volcanology and Geothermal Research 392, 106763. https://doi.org/10.1016/j.jvolgeores.2019.106763

Hayes, J.L., Wilson, T.M., Magill, C., 2015. Tephra fall clean-up in urban environments. Journal of Volcanology and Geothermal Research 304, 359–377. https://doi.org/10.1016/j.jvolgeores.2015.09.014

Hopkins, J.L., Smid, E.R., Eccles, J.D., Hayes, J.L., Hayward, B.W., McGee, L.E., van Wijk, K., Wilson, T.M., Cronin, S.J., Leonard, G.S., Lindsay, J.M., Németh, K., Smith, I.E.M., 2021. Auckland Volcanic Field magmatism, volcanism, and hazard: a review. New Zealand Journal of Geology and Geophysics 64, 213–234. https://doi.org/10.1080/00288306.2020.1736102

Houghton, B.F., Bonadonna, C, Gregg, C.E., Johnston, D.M., Cousins, W.J., Cole, J.W., Del Carlo, P., 2006. Proximal tephra hazards: Recent eruption studies applied to volcanic risk in the Auckland volcanic field, New Zealand. Journal of Volcanology and Geothermal Research 155(1-2), 138-149. https://doi.org/10.1016/j.jvolgeores.2006.02.006

Hovey, E.O., 1904. The 1902-1903 Eruptions of Mont Pelé, Martinique and the Soufrière, St. Vincent. Brothers Hollinek.

Jenkins, S., Baxter, P.J., Spence, R., Purser, D., Brown, A., 2009. Fire potential following pyroclastic flow in the Vesuvius area (Technical report for project SPeeD). Cambridge Architectural Research.

Jenkins, S.F., Day, S.J., Faria, B.V.E., Fonseca, J.F.B.D., 2017. Damage from lava flows: insights from the 2014–2015 eruption of Fogo, Cape Verde. Journal of Applied Volcanology 6, 6. https://doi.org/10.1186/s13617-017-0057-6

Jenkins, S.F., Spence, R.J.S., Fonseca, J.F.B.D., Solidum, R.U., Wilson, T.M., 2014. Volcanic risk assessment: Quantifying physical vulnerability in the built environment. Journal of Volcanology and Geothermal Research 276, 105–120. https://doi.org/10.1016/j.jvolgeores.2014.03.002

Jenkins, S., Komorowski, J.-C., Baxter, P.J., Spence, R., Picquout, A., Lavigne, F., Surono, 2013. The Merapi 2010 eruption: An interdisciplinary impact assessment methodology for studying pyroclastic density current dynamics. Journal of Volcanology and Geothermal Research 261, 316–329. https://doi.org/10.1016/j.jvolgeores.2013.02.012

Jenkins, S.F., Komorowski, J.-C., Baxter, P.J., Charbonnier, S.J., Cholik, N., Surono, 2016. The Devastating Impact of the 2010 Eruption of Merapi Volcano, Indonesia, in: Duarte, J.C., Schellart, W.P. (Eds.), Geophysical Monograph Series. John Wiley & Sons, Inc., Hoboken, NJ, USA, pp. 259–269. https://doi.org/10.1002/9781119054146.ch12

Ju, W., 2016. Study on Fire Risk and Disaster Reducing Factors of Cotton Logistics Warehouse Based on Event and Fault Tree Analysis. Procedia Engineering, 2015 International Conference on Performance-based Fire and Fire Protection Engineering (ICPFFPE 2015) 135, 418–426. https://doi.org/10.1016/j.proeng.2016.01.150

Kilburn, C.R.J., 2015. Chapter 55 - Lava Flow Hazards and Modeling, in: Sigurdsson, H. (Ed.), The Encyclopedia of Volcanoes (Second Edition). Academic Press, Amsterdam, pp. 957–969. https://doi.org/10.1016/B978-0-12-385938-9.00055-9

Lacroix, A., 1904. La Montagne Pelee et ses eruptions. Masson.

Lee, S., Davidson, R., Ohnishi, N., Scawthorn, C., 2008. Fire following Earthquake—Reviewing the State-of-the-Art of Modeling: Earthquake Spectra 24, 933–967. https://doi.org/10.1193/1.2977493

Leonard, G.S., Calvert, A.T., Hopkins, J.L., Wilson, C.J.N., Smid, E.R., Lindsay, J.M., Champion, D.E., 2017. High-precision 40Ar/39Ar dating of Quaternary basalts from Auckland Volcanic Field, New Zealand, with implications for eruption rates and paleomagnetic correlations. Journal of Volcanology and Geothermal Research 343, 60–74. https://doi.org/10.1016/j.jvolgeores.2017.05.033

Lerner, G.A., Jenkins, S.F., Charbonnier, S.J., Komorowski, J.-C., Baxter, P.J., 2022. The hazards of unconfined pyroclastic density currents: A new synthesis and classification according to their deposits, dynamics, and thermal and impact characteristics. Journal of Volcanology and Geothermal Research 421, 107429. https://doi.org/10.1016/j.jvolgeores.2021.107429

Longpré, M.-A., 2021. Reactivation of Cumbre Vieja volcano. Science. https://doi.org/10.1126/science.abm9423

Magill, C., Blong, R., McAneney, J., 2006. VolcaNZ—A volcanic loss model for Auckland, New Zealand. Journal of Volcanology and Geothermal Research 149, 329–345. https://doi.org/10.1016/j.jvolgeores.2005.09.004

Mastin, L.G., 2001. A simple calculator of ballistic trajectories for blocks ejected during volcanic eruptions (Open-File Report No. 01–45). U.S. Geological Survey.

McDonald, G.W., Smith, N.J., Kim, J., Cronin, S.J., Proctor, J.N., 2017. The spatial and temporal 'cost' of volcanic eruptions: assessing economic impact, business inoperability, and spatial distribution of risk in the Auckland region, New Zealand. Bull Volcanol 79, 48. https://doi.org/10.1007/s00445-017-1133-9

Meredith, E.S., Jenkins, S.F., Hayes, J.L., Deligne, N.I., Lallemant, D., Patrick, M., Neal, C., 2022. Damage assessment for the 2018 lower East Rift Zone lava flows of Kīlauea volcano, Hawaiʻi. Bull Volcanol 84, 65. https://doi.org/10.1007/s00445-022-01568-2

Nakada, S., Shimizu, H., Ohta, K., 1999. Overview of the 1990–1995 eruption at Unzen Volcano. Journal of Volcanology and Geothermal Research 89, 1–22. https://doi.org/10.1016/S0377-0273(98)00118-8

Needham, A.J., Lindsay, J.M., Smith, I.E.M., Augustinus, P., Shane, P.A., 2011. Sequential eruption of alkaline and sub-alkaline magmas from a small monogenetic volcano in the Auckland Volcanic Field, New Zealand. Journal of Volcanology and Geothermal Research, From maars to scoria cones: the enigma of monogenetic volcanic fields 201, 126–142. https://doi.org/10.1016/j.jvolgeores.2010.07.017

Németh, K., Cronin, S.J., Smith, I.E.M., Agustin Flores, J., 2012. Amplified hazard of small-volume monogenetic eruptions due to environmental controls, Orakei Basin, Auckland Volcanic Field, New Zealand. Bulletin of Volcanology 74, 2121-2137. https://doi.org/10.1007/s00445-012-0653-6

Paté-Cornell, M.E., 1984. Fault Trees vs. Event Trees in Reliability Analysis. Risk Analysis 4, 177–186. https://doi.org/10.1111/j.1539-6924.1984.tb00137.x

Paulik, R., Horspool, N., Woods, R., Griffiths, N., Beale, T., Magill, C., Wild, A., Popovich, B., Walbran, G., Garlick, R., 2022. RiskScape: A flexible multi-hazard risk modelling engine (preprint). In Review. https://doi.org/10.21203/rs.3.rs-1123016/v1

Pistolesi, M., Delle Donne, D., Pioli, L., Rosi, M., Ripepe, M., 2011. The 15 March 2007 explosive crisis at Stromboli volcano, Italy: Assessing physical parameters through a multidisciplinary approach. Journal of Geophysical Research: Solid Earth 116. https://doi.org/10.1029/2011JB008527

Runge, M.G., Bebbington, M.S., Cronin, S.J., Lindsay, J.M., Moufti, M.R., 2015. Sensitivity to volcanic field boundary. J Appl. Volcanol. 4, 22. https://doi.org/10.1186/s13617-015-0040-z

Scawthorn, C., 2018. Fire following the Mw 7.05 Haywired earthquake scenario. Los Angeles 12.

Scawthorn, C., 1986. Fire Following Earthquake. Fire Safety Science 1. https://doi.org/10.3801/IAFSS.FSS.1-971

Scawthorn, C., Eidinger, J.M., Schiff, A., 2005. Fire Following Earthquake. ASCE Publications.

Scheele, F.R., Horspool, N.A., 2018. Modelling fire following earthquake in Wellington : a review of globally available methodologies (No. 2017/42). GNS Science, Lower Hutt (NZ).

Scheele, F.R., Lukovic, B., Horspool, N.A., 2019. Revisiting fire following earthquake modelling for Wellington City (No. 2019/24). GNS Science, Lower Hutt (NZ).

Simpson, A., Murnane, R., Saito, K., Phillips, E., Reid, R., Himmelfarb, A., 2014. Understanding Risk in an Evolving World: Emerging Best Practices in Natural Disaster Risk Assessment (International Strategy for Disaster Reduction). Global Facility for Disaster Reduction and Recovery, The World Bank, UN, Washington, DC.

Stats NZ, 2021. Auckland Region (Subnational population estimates: At 30 June 2021 (provisional)), Information releases. Stats NZ.

Stats NZ, 2020. Regional gross domestic product: Year ended March 2019 (Information releases). Stats NZ.

Stewart, C., Johnston, D.M., Leonard, G.S., Horwell, C.J., Thordarson, T., Cronin, S.J., 2006. Contamination of water supplies by volcanic ashfall: A literature review and simple impact modelling. Journal of Volcanology and Geothermal Research 158, 296–306. https://doi.org/10.1016/j.jvolgeores.2006.07.002

Suwondo, R., Cunningham, L., Gillie, M., Bailey, C., 2019. Progressive collapse analysis of composite steel frames subject to fire following earthquake. Fire Safety Journal 103, 49–58. https://doi.org/10.1016/j.firesaf.2018.12.007

Tanguy, J.-C., 1994. The 1902–1905 eruptions of Montagne Pelée, Martinique: anatomy and retrospection. Journal of Volcanology and Geothermal Research 60, 87–107. https://doi.org/10.1016/0377-0273(94)90064-7

Thomas, G.C., Schmid, R., Cousins, W.J., Heron, D.W., Lukovic, B., 2006. Post-Earthquake Fire Spread between Buildings – Correlation with 1931 Napier Earthquake, in: Proceeds of the New Zealand Society for Earthquake Engineering Annual Conference. Napier, p. 8.

Thomas, R.M.E., Sparks, R.S.J., 1992a. Cooling of tephra during fallout from eruption columns. Bull Volcanol 54, 542–553. https://doi.org/10.1007/BF00569939

Tsunematsu, K., Ishimine, Y., Kaneko, T., Yoshimoto, M., Fujii, T., Yamaoka, K., 2016. Estimation of ballistic block landing energy during 2014 Mount Ontake eruption. Earth, Planets and Space 68, 88. https://doi.org/10.1186/s40623-016-0463-8

Turchi, A., Di Traglia, F., Luti, T., Olori, D., Zetti, I., Fanti, R., 2020. Environmental Aftermath of the 2019 Stromboli Eruption. Remote Sensing 12, 994. https://doi.org/10.3390/rs12060994

Vanderkluysen, L., Harris, A.J.L., Kelfoun, K., Bonadonna, C., Ripepe, M., 2012. Bombs behaving badly: unexpected trajectories and cooling of volcanic projectiles. Bull Volcanol 74, 1849–1858. https://doi.org/10.1007/s00445-012-0635-8

Wang, Y., Gibson, L., Beshir, M., Rush, D., 2021. Determination of Critical Separation Distance Between Dwellings in Informal Settlements Fire. Fire Technol 57, 987–1014. https://doi.org/10.1007/s10694-020-01075-w

Wardman, J., Sword-Daniels, V., Stewart, C., Wilson, T., 2012b. Impact assessment of the May 2010 eruption of Pacaya volcano, Guatemala, GNS Science Report. GNS Science, Lower Hutt, N.Z.

Wardman, J.B., Wilson, T.M., Bodger, P.S., Cole, J.W., Stewart, C., 2012a. Potential impacts from tephra fall to electric power systems: a review and mitigation strategies. Bull Volcanol 74, 2221–2241. https://doi.org/10.1007/s00445-012-0664-3

Williams, G.T., Kennedy, B.M., Wilson, T.M., Fitzgerald, R.H., Tsunematsu, K., Teissier, A., 2017. Buildings vs. ballistics: Quantifying the vulnerability of buildings to volcanic ballistic impacts using field studies and pneumatic cannon experiments. Journal of Volcanology and Geothermal Research 343, 171–180. https://doi.org/10.1016/j.jvolgeores.2017.06.026

Williams, R.S., Moore, J.G., 1983. Man Against Volcano: The Eruption in Heimaey, Vestmannaeviar, Iceland. U.S. Geological Survey.

Williamson, R., Groner, N., 2000. Ignition of fires following earthquakes associated with natural gas and electric distribution systems. Pacific Earthquake Engineering Research Center, Berkeley, CA.

Wilson, G., Wilson, T.M., Deligne, N.I., Blake, D.M., Cole, J.W., 2017. Framework for developing volcanic fragility and vulnerability functions for critical infrastructure. Journal of Applied Volcanology 6, 14. https://doi.org/10.1186/s13617-017-0065-6

Wilson, G., Wilson, T.M., Deligne, N.I., Cole, J.W., 2014. Volcanic hazard impacts to critical infrastructure: A review. Journal of Volcanology and Geothermal Research 286, 148–182. https://doi.org/10.1016/j.jvolgeores.2014.08.030

Wilson, T.M., Cole, J.W., 2007. Potential impact of ash eruptions on dairy farms from a study of the effects on a farm in eastern Bay of Plenty, New Zealand; implications for hazard mitigation. Nat Hazards 43, 103–128. https://doi.org/10.1007/s11069-007-9111-8

Wilson, T.M., Stewart, C., Sword-Daniels, V., Leonard, G.S., Johnston, D.M., Cole, J.W., Wardman, J., Wilson, G., Barnard, S.T., 2012. Volcanic ash impacts on critical infrastructure. Physics and Chemistry of the Earth, Parts A/B/C, Volcanic ash: an agent in Earth systems 45–46, 5–23. https://doi.org/10.1016/j.pce.2011.06.006

Yildiz, S.S., Karaman, H., 2013. Post-earthquake ignition vulnerability assessment of Küçükçekmece District. Natural Hazards and Earth System Sciences 13, 3357–3368. https://doi.org/10.5194/nhess-13-3357-2013

Youance, S., Nollet, M.-J., McClure, G., 2012. Post-earthquake functionality of critical facilities: A hospital case study. Lisboa, p. 10.

Zolfaghari, M.R., Peyghaleh, E., Nasirzadeh, G., 2009. Fire Following Earthquake, Intra-structure Ignition Modeling. Journal of Fire Sciences 27, 45–79. https://doi.org/10.1177/0734904108094516

Zuccaro, G., De Gregorio, D., Baxter, P., 2015. Chapter 10 - Human and Structural Vulnerability to Volcanic Processes, in: Shroder, J.F., Papale, P. (Eds.), Volcanic Hazards, Risks and Disasters. Elsevier, Boston, pp. 261–288. https://doi.org/10.1016/B978-0-12-396453-3.00010-1